Passive acoustic monitoring in the outer Bay of Fundy, and assessment of communication space loss in right whales.

Final Report

Prepared by:

Kalen Mawer, Kirsti Mrazek

Passive acoustic monitoring in the outer Bay of Fundy, and assessment of communication space loss in right whales.

Kalen Mawer*, Kirsti Mrazek

Aquatic Science Program Manager
kmawer@ecw.ngo

March, 2024

With excerpts from documents written by Joseph P. Sharman, Lee Penney, and Robert White

Published by:
Eastern Charlotte Waterways Inc.
881 Main Street
Blacks Harbour, NB
Canada, E5H 1E5
Tel: (506) 456-6001
Fax: (506) 456-6187
E-mail: info@ecw.ngo
Web: www.ecw.ngo

This project has been made possible by the financial support of:

Fisheries and Oceans Canada | Pêches et Océans Canada

Canada

Table of Contents

1.0. Executive Summary

Recent rising levels of global shipping have increased pressure on marine mammals through underwater noise pollution around ports and shipping lanes, causing impacts on species fitness by masking communication spaces and displacing individuals from critical habitats. Quantifying where and how much sound is distributed throughout marine environments through regionally-accurate sound propagation models are critical in effective management and mitigation of the potential impacts from underwater noise. Seasonal populations of North Atlantic Right Whale (NARW; *Eubalaena glacialis*) in the outer Bay of Fundy are protected under the federal Species at Risk Act in Canadian waters, along with a spatial management zone for their critical habitat. These whales are known to communicate in a wide frequency range (appx. 50 - 3000 Hz), overlapping with vessel noise and other anthropogenic activities. The critical habitat is located adjacent to the Bay of Fundy Traffic Separation Scheme (shipping lane); therefore, monitoring anthropogenic noise levels in this area is vital for conservation of this species.

This report delivers results of this multi-year project for monitoring noise pollution levels from shipping in the outer Bay of Fundy (OBF). Through this project, passive acoustic monitoring was used both to calculate a rate of spreading loss for the outer Bay of Fundy and to record vessels leaving Port Saint John which generated a dataset of specific ship signatures. A model was designed which, through the input of vessel noise and specifics of marine mammal communication, visualizes spreading loss and inhibition to marine mammal communication. The data collected through passive acoustic monitoring, alongside additional data collected by ECW since 2015, also contributes to a larger dataset currently being used to understand spatiotemporal patterns in marine mammals.

Passive acoustic monitoring (PAM) was used to collect broadband waveform sound data from hydrophones at four sites in the outer Bay of Fundy. In the first phase, PAM data was used to calculate a coefficient of spreading loss for two vessels (a ferry and a container ship), which was used in combination with environmental data to model transmission loss in the Bay of Fundy. In the second phase, PAM data collected adjacent to the Traffic Separation Scheme was used to develop noise signatures for five classes of vessel (cruise ships, oil tankers, petroleum tankers, potash ships, and container ships) at various relevant ⅓ octave bands, which were run through the model to understand the way their associated noise propagates. An overlay demonstrates communication space loss for multiple species of marine mammals. Cruise ships at the 125 Hz ⅓ octave band were found to have the greatest effect on NARW and Humpback whale (*Megaptera novaeangliae*) communication space, where a one kilometer radius around the vessel could cause high to moderate inhibition to communication. Many of the analyzed ship signatures at multiple ⅓ octave bands had little to no effect on communication space for other species.

The models are limited in their capacity by the ability to model only one vessel at a time, and to model along a single two dimensional transect. Model outputs could be improved by better information on marine mammal communication in this region. Further work should focus on making the models more useful for users through front-end development and better ability to model, radially, and in real-time. Despite these limitations, the models can serve as a good foundation for understanding how noise may affect communication space loss in baleen whales in the Bay of Fundy.

2.0. Introduction

Marine environments provide some of the most complex and important ecosystem services worldwide. Over the last few decades increased rates of global shipping have increased the risks to the physiology and ecology of marine life from heightened levels of vessel traffic around ports and shipping lanes. Marine mammals are one group which face increased impacts from the expansion of global shipping. Ship strikes killing whales is a common problem in some areas leading to stringent, and often quickly implemented, management measures to mitigate this issue. Underwater noise pollution is also a primary concern, albeit less immediately noticeable and the effects of which are more challenging to understand. Marine mammals use sound for communication, foraging, social interactions, and courtship (Erbe et al, 2019). Therefore, increased anthropogenic noise at certain frequencies can mask sounds and communication spaces for marine mammals, altering critical life functions and can even displace whole populations from known feeding or breeding areas, causing dramatic impacts on life history strategy, fitness and fecundity (Richardson et al, 1995).

Underwater noise produced by shipping has been identified as one of the main inputs of noise pollution to marine ecosystems (Zhang et al, 2020); quantifying the levels and distribution of sound spatiotemporally and generating accurate acoustic sound propagation models are critical to mapping the extent of noise pollution. However, sound propagation in marine systems is directly related to the physical conditions of the environment, meaning that broad assumptions of how noise interacts with marine ecosystems are often unfounded. Developing regional models of sound propagation requires understanding the rate of underwater spreading loss (or transmission loss), the rate at which sound dissipates through the aquatic medium. Spreading loss will change regionally based on depth and other physical characteristics of the environment, however, sound propagation models often assume a value (a coefficient) for depth from which to calculate spreading loss. Modelling how underwater noise from shipping, at specific frequencies and different amplitudes, propagates and dissipates in local environments is vital to understanding how to manage noise pollution under regional management strategies, especially with consideration to species at risk.

North Atlantic Right Whale (NARW; *Eubalaena glacialis*) populations have been designated as 'threatened' and have been protected in Canadian waters under the Species at Risk Act (SARA) since 2005, meaning they are a protected species under federal law, managed under the framework of a recovery strategy with specific conservation objectives. Two areas of critical habitats for *E. glacialis* were subsequently identified and protected in eastern Canadian waters as part of conservational management measures established by the Department of Fisheries and Oceans Canada (DFO). These areas include the Roseway Basin, off the southeastern coast of Nova Scotia and the Grand Manan Basin in the outer Bay of Fundy. The main threats to *E. glacialis* populations in Canadian waters have been identified as: entanglement in fishing gear, collisions with large vessels, and underwater noise pollution.

In 2018 Eastern Charlotte Waterways Inc. (ECW), in partnership with Dr. Jack Terhune at the University of New Brunswick, was awarded funding for this project to assess underwater noise pollution levels around the critical habitat of the North Atlantic Right Whale (*Eubalaena glacialis*), which are at high risk to adverse impacts from shipping noise through masking of acoustic communication space and displacement from the Grand Manan critical habitat. Monitoring noise pollution levels in the Bay of

Fundy is also of current interest because of the ongoing expansion of the Port of Saint John, which was aiming to increase its previous capacity by over 200% by 2023 and be able to facilitate larger vessels. This project aims to use passive acoustic monitoring techniques to assess underwater noise levels in the outer Bay of Fundy, seeking to model noise levels in order to develop working models of underwater sound propagation, and couple underwater noise recordings with specific ships operating in the bay to calculate a regional rate of spreading loss of shipping noise at various frequencies. Achieving these aims will facilitate further understanding of levels of potential communication space masking in North Atlantic Right Whales.

This document provides a final report for this project, summarizing the passive acoustic monitoring (PAM) data collected throughout the project, explaining the models built to simulate transmission loss of underwater noise in the outer Bay of Fundy, and demonstrating the application of those models using real data of ships traveling from Port Saint John.

3.0. Methodology

3.1. Study area

The outer Bay of Fundy (OBF) is the lower (southwestern) half of the Bay of Fundy. It is the area that connects the inner bay to the Gulf of Maine and is characterized by high tidal flow and heightened levels of benthic biodiversity (Buzeta and Singh, 2008). There are many islands present in the OBF, the largest of which is Grand Manan. These islands create a structurally complex and dynamic region which supports an extensive and biodiverse marine trophic system. Large populations of marine mammals can be found in the OBF, including seals, dolphins, porpoises and large baleen whales. Baleen whale presence in the OBF is seasonal as populations migrate from southern wintering grounds to feed in the Bay of Fundy. These species include the endangered North Atlantic Right Whale which can be found in the area from late summer into fall.

The OBF is economically important and includes areas for commercial fishing, aquaculture, wildlife watching, and other recreational and cultural activities. The OBF also includes Canada's third largest commercial shipping port and fourth largest cruise ship dock, with a designated commercial shipping lane: Port Saint John. This shipping lane was altered from its original location in 2002 to support conservation and management efforts for right whales by avoiding their critical habitat. However, the shipping lane still remains close to the NARW critical habitat, and therefore, monitoring of the impacts of commercial shipping activities in the Bay of Fundy remains critical to the successful conservation of this endangered species.

3.2. Passive acoustic monitoring methods

Sampling for passive acoustic monitoring (PAM) was conducted in several locations. Monitoring events in 2019 and 2020 were conducted with a single-hydrophone system at three sites: Grand Manan

(44.64765° N, -66.62865° W), in Dipper Harbour (45.048950° N, -66.445540° W), and in the Saint John Harbour (45.223360° N, -66.080130° W)(Figure 1, Table 1). In 2021 and 2022, three deployments were made using a new vertical hydrophone array, at theTraffic Separation Scheme (TSS) site (45.014783° N, -66.199567° W)(Figure 1, Table 1). As the hydrophone array was designed in adherence with the ISO-17208-1 standard (International Organization for Standardization [ISO], 2016), it was deployed in over 90m of water approximately 80m away from the outgoing lane of the traffic separation scheme.

In the initial proposal, an additional site was anticipated to be established through this project. It would have been adjacent to the incoming shipping lane, outside of Digby, NS. This was not possible due to logistical constraints including delays in receipt of necessary equipment and restriction in project activities during the COVID-19 pandemic, as well as funding constraints caused by the increased cost of running the PAM hydrophone array after having switched to lithium batteries. Fortunately, the establishment of the TSS site proved more useful than a Digby site would have been in the later phases of the project.

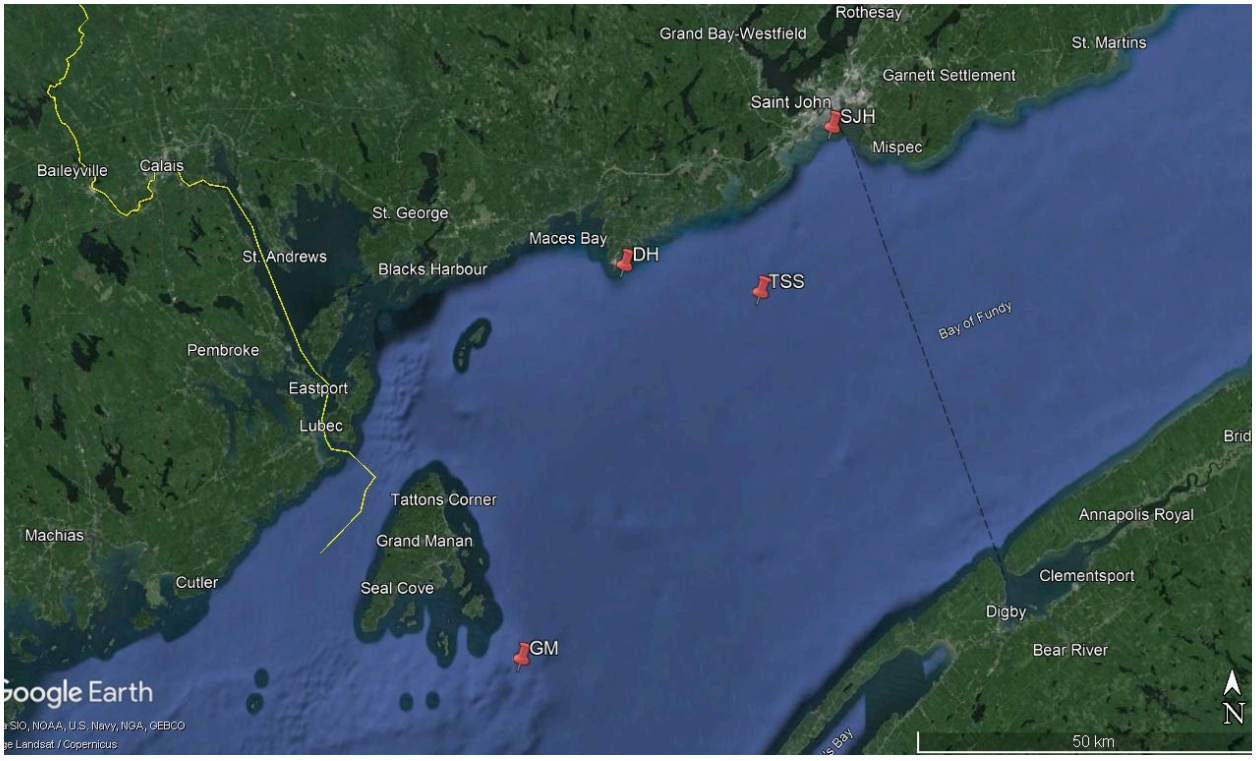

Figure 1. Map of passive acoustic monitoring locations: Saint John Harbour (SJH), Dipper Harbour (DH), Grand Manan (GM) and adjacent to the outgoing lane of the Traffic Separation Scheme (TSS).

Table 1. Specifics (date of deployment and site name) for project hydrophone deployments in the Bay of Fundy from 2019-2022.

Year	Site	Deployment Dates
2019	Saint John Harbour	June 26
		October 21
	Grand Manan	June 11
		August 1
		October 3
	Dipper Harbour	July 18
		September 12
2020	Saint John Harbour	January 28
		March 12
	Dipper Harbour	July 21
	Grand Manan	July 22
		September 9
2021	Traffic Separation Scheme (TSS)	October 7
2022	Traffic Separation Scheme (TSS)	August 10
		September 13

3.2.1. Equipment

Ocean Sonics icListen HF Hydrophones were used for PAM at all sites. These devices measure 26.3cm and are manufactured in Nova Scotia. All hydrophones were set to record noise data in both .wav and FFT (Fast Fourier Transform) formats, recording between the frequencies of 10Hz and 20,000Hz. For the current study, however, only the waveform data was used. Sampling rates were set to 32ks/s, a setting consistent with data collection for other projects at ECW prior to 2019. Power was regulated through the use of Gordon Smart Board, contained within the Subsea Battery Pack (Ocean Sonics). Power levels were checked digitally through the Gordon software prior to deployments to ensure maximum energy capacity for the deployment. The battery pack was then bolted securely into a metal 'In-Line Battery Pack Frame (Ocean Sonics), which was attached to anchors (150-220lbs) at the bottom and a series of flotation buoys at the top to hold the hydrophone upright vertically in the water column. Finally, an acoustic release system (Vemco VR2AR) was included between the anchor chain and the battery pack, for use to detach the hydrophone, battery pack, and buoys from the anchors to retrieve equipment; the acoustic release was activated using a surface-to-receiver communications receiver and transponding hydrophone (Vemco VR100). All components of the hydrophone system were then placed in-line and secured together using metal cabling, ropes, Crosby clips, shackles, and cable ties.

Power was supplied to the hydrophones by a titanium battery pack (Ocean Sonics – Subsea Battery Pack) which housed 72 industrial grade D-cell alkaline batteries, consistent with earlier deployments made by ECW. In 2021, one battery pack unit was modified by OceanSonics to support a three-hydrophone ISO-17208-1-compliant (ISO, 2016) array as opposed to a single hydrophone. Modifications included the addition of two ports at the top of the battery pack and the conversion to lithium battery power in hopes of prolonging the number of days recorded per deployment. The rest of the deployment in-line system

for the array was similar to that used in previous years for single-hydrophone deployments, with the exception of two additional hydrophones placed along over 70m of line and cable between the battery pack and the buoys. The hydrophones were fixed to the lines at 46m, and 21.5m, in addition to one on the battery pack at 80m, to adhere to specifications in the ISO standards (ISO, 2016). All data were recorded on an external 2TB hard drive as opposed to the internal hydrophone storage.

3.2.2. Deployments & retrievals

Hydrophone systems were first programmed for deployment in the ECW office by synchronizing the internal clock in the hydrophone to correct UTC time zone using a computer, selecting a sample rate for both waveform and FFT data, selecting a delayed start time (chosen to activate close to the expected time of deployment) and by ensuring the hydrophone is active and being correctly read by the Gordon system. Finally, a duty cycle was set allowing the hydrophone system to conserve battery power by recording only for a set amount of time. For this project a duty cycle of 5/20 was set, meaning the hydrophone would record data for 5 minutes every 20 minutes for each deployment. The result was 15 minutes of data every hour or 360 minutes of data per active day during a sampling deployment. Acoustic releases were primed and checked at this stage prior to deployment. Based on the product specifications for battery power and SSD storage capacity from the manufacturer, deployments were estimated to last less than 5 weeks.

Most deployments were conducted with the help of a fishing vessel, where ECW staff worked with vessel crew. Site coordinates were input in the vessel navigation system. For single-hydrophone deployments: the anchor chain was secured to a cleat on the vessel with a rope, the buoys and lines were laid out on the deck, the buoys and lines were released into the water while the boat steamed ahead gently, and once the lines were straight the anchor tether was cut allowing the anchor to sink. Two to three ECW staff were sufficient for these deployments, with one crew member from the fishing vessel alongside the captain. With so much additional line, the hydrophone array was more challenging to deploy, needing the use of a skiff along with the fishing vessel. Once on site the skiff would carry the buoys while the fishing vessel had the connected lines and anchor, which was tethered to the vessel in the same way as single-hydrophone deployments. The skiff reversed away from the fishing vessel and drew out the lines while staff on deck ensured they did not tangle. When all the lines were in the water between the skiff and the fishing vessel, the buoys were released from the skiff and then the anchor was cut from the tether on the fishing vessel. Five to six ECW staff worked on these deployments, alongside the one crew member from the fishing vessel and the vessel captain. In both cases, new coordinates were taken after the anchor was cut in an attempt to account for any wind or currents that caused the boat or equipment to move off site. This facilitated the retrievals. Retrievals were mainly conducted with an ECW skiff and three staff, but were conducted on a fishing vessel if there would be inclement weather. The skiff or fishing vessel traveled to the site marked during deployment and triggered the acoustic release using the VEMCO VR100 receiver. Staff then scanned the water and listened for the splash of the buoys surfacing. When found, the vessel would travel to the buoys, lift them into the boat using a gaff, and pull the lines in by hand.

3.2.3. Waveform sound analysis

Once retrieved, data from hydrophone deployments were uploaded to a computer and stored on two separate hard drives for storage and backup. Waveform data was then processed and analyzed using noiseLAB Pro Capture (v.4.0.4; DELTA, 2014) to calculate sound levels for each 1/3 octave frequency band from 10 to 125000Hz. These 1/3 octave outputs were then calibrated using a value calculated by testing the hydrophone against a steady tone from a known frequency, done in a lab-like setting at the ECW office in Blacks Harbour in March 2019. The value calculated for calibration was similar for all hydrophones tested at 86 dB (±1), therefore the value of 86 was used for all.

From the 2019 deployments, sound levels for 1/3 octave calculations were analyzed spatially and temporally in R (R Core Team, 2019) to assess the distribution of underwater noise levels for known 1/3 octave bands, quantified using amplitude as decibels (dB) relative to 1 micropascal (re 1 µPa). Bands 63 Hz and 125 Hz were assessed, as these are the bands associated with underwater noise pollution from industrial shipping by the European Union's Marine Strategy Framework Directive (European Union [EU], 2008). 1/3 octave bands 20 Hz and 1000 Hz are also being assessed as they are associated with communication ranges for baleen whales and other marine vessels, respectively. The MSFD aims to keep amplitudes at the 63Hz and 125Hz bands <100 dB re 1 µPa. European regulatory frameworks were used as the basis for this assessment as Canadian regulations for assessment of underwater noise pollution from shipping are still being developed. These results were not included in this report as they were not included in the modelling and communication inhibition analysis.

The data collected from this project is currently being used to assess marine mammal occurrence. JASCO Applied Sciences was contracted to process the waveform data and apply automated marine mammal detectors to each recording. One of the acoustic metrics calculated during the data processing was sound pressure level (SPL_{rms}, dB re 1 µPa s)(Lawrence, C.B. 2023). The one minute average sound pressure level values were used to calculate the average sound pressure levels over the course of each deployment. Each five minute recording was manually analyzed and validated for marine mammal call identification.

3.3. Methods for understanding sound propagation

3.3.1. Calculating spreading loss

Spreading loss is calculated in two ways, the first is for spherical spreading loss, which is used for deep water where transmission from the sound source is assumed to spread uniformly in all directions, unrestricted by the surface or the bottom, radiating as a sphere. The second is for cylindrical spreading loss, which is used for shallow water, where the sound transmission from the source is contained within reflective layers (usually trapped between the surface and the seafloor) forcing sound to radiate in a cylindrical manner. Often in nature sound propagation starts with spherical spreading loss for a certain distance and then becomes cylindrical spreading as sound hits the surface and seafloor. Both forms of spreading are calculated using the following equations, where R = range and R_0 = the reference range (1 meter):

Equation 1:

Spherical spreading loss = 20 log [R/R_0]

Equation 2:

Cylindrical spreading loss = 20 log R, + 10 log [R/R_0]

A predefined coefficient (**K**) is used in the calculation of spreading loss, in the equations above K is 20 for spherical spreading loss and 10 for cylindrical spreading loss, 15 is often used for both. However, these values are optimized from global data and are not specific to localized geographic regions and therefore are not accurate and could vary depending on physical environmental conditions locally. To calculate spreading loss regionally, a local value for K is needed. Therefore, to calculate spreading loss in the OBF we must first establish a local calculation for K.

Establishing a value for the rate of spreading loss in the outer Bay of Fundy was achieved through first obtaining Automatic Identification System (AIS) data for the region during the 2019 hydrophone deployments; this data was purchased through exactEarth. AIS data was then filtered (using ESRI ArcGIS) for the most frequent vessels which were moving during active recording periods of hydrophone deployments, resulting in a list of vessels and their exact positions during hydrophone deployment times. 1/3 octave outputs generated by noiseLAB Pro Capture (v4.0.4; DELTA, 2014) were then processed through a separate software, noiseLAB Pro Batch (v4.1; DELTA, 2015) to break down the time scale of the sound level assessment into 10-second time slices, resulting in an individual 1/3 octave sound level recording for a 10 second period of time. These 10 second slices were then aligned with the known locations of the vessels to give an exact reading of amplitude around the vessel. This was done for the entire track of the vessel as it came by a hydrophone, resulting in a track of 10 second sound level readings as the vessel moved through the water. These sound level amplitudes (y) were then modeled against the vessel's distance from the hydrophone (x), producing a scatter plot of sound levels for any given 1/3 octave band, calculating a relationship between amplitude and distance (K). A Microsoft Excel Solver add-in was then used to estimate an optimized, regional K value from the observed data in the scatterplot, by comparing the errors from a predicted K value in the model, resulting in a calculation of spreading loss (K) specific to the outer Bay of Fundy.

Two vessels were chosen to assess spreading loss because of their frequency passing the hydrophone, allowing for high sample rates of data and allowing for strength in the model. These vessels were The Fundy Rose (IMO: 9203916), the 124m and 10,000 tonne ferry which operates daily and sometimes twice daily, between Saint John, NB and Digby, NS, and the MSC Tamara (IMO: 9351579), a 264m and 41,000 tonne container ship which made several passages within the hydrophone active periods. The Fundy Rose was selected for analysis as it made regularly scheduled trips across the OBF and was therefore a reliable (frequent) source of data during active hydrophone periods. However, high levels of interference from other vessels were observed in the models and therefore, interference was identified and removed from the subsequent analysis with the MSC Tamara to assess if this aided in generating a more accurate model.

3.3.2. Modelling sound propagation

The following is a brief summary of the methods used to model spreading loss in the outer Bay of Fundy. The full details of this work and example simulations can be found in Appendix A.

RAMGeo and RAMSGeo are underwater acoustic propagation models that can handle low frequencies and range-dependent environments; the former treats the seafloor as a fluid whereas the latter accounts for the shear forces in the seafloor by treating it as an elastic. Both generate numerical solutions to the wave equation in the form of an outgoing cylindrical wave that is propagating energy at small angles to the horizontal by utilizing a split-step Padé algorithm. The models are only capable of handling one frequency at a time. Each model requires an environment file which defines the physical and numerical properties of the ocean environment along a particular azimuth from the sound source, as well as properties of the sound source. Physical parameters include the bathymetry and sound speed profile in the ocean, as well as material properties, such as density and attenuation, of the solid layers below the seafloor. The two acoustic source parameters are the frequency of the sound source in Hertz and the depth of the sound source in meters. All the ocean, acoustic, and numerical information are written to an environment file in MATLAB. Transmission loss is then computed using the acoustic model of choice. Three zones of inhibition level to marine mammal communication, high inhibition, medium inhibition, and low inhibition, are computed from transmission loss and two marine mammal hearing threshold values (see section 3.3.4); these are overlain on the original output.

3.3.3. Ship signatures

Ship-specific noise signatures were calculated using the 2021 and 2022 deployments. Data on departure dates and times from Port Saint John was retrieved from their website (Port Saint John, 2023).

Tidal strum masked much of the noise in the mid-level and top-level hydrophones; data from the bottom (deepest) hydrophone (attached directly to the battery pack) was used for this analysis. The noise level was graphed at the 20, 63, 125, 1000, and 12500 ⅓ octave bands over time (Figure 2) which was visually inspected for peaks which matched up with the departures from the port. Noise signatures in the 20 and 125000 Hz ⅓ octave bands were originally calculated and graphed, however were omitted from analyses and modelling as they did not appear to change when passing vessels were identified. Despite use of the deepest hydrophone, some passing vessels were partially or completely masked during times when tides were moving the quickest. The 63 and 125 Hz ⅓ octave bands demonstrated the most drastic peaks when ships passed, and thus were used primarily in comparison with the vessel departures. Occasionally, the 63 and 125 Hz ⅓ octave bands would experience separate peaks (20 minutes apart as per the duty cycle), in which case the peak in the 1000 Hz ⅓ octave band was used to determine which time (and thus, which data) would be used in the analysis. There were also times when two ships would leave the port around the same time, and the peaks would show up close together on the graph. These were excluded from the analysis in case of an event where one vessel passed the other before passing by the hydrophone.

The identified ships were grouped into the following categories based on the information provided from the port departures website: container, cruise, potash, petroleum, crude oil, recycled metal, fish oil,

equipment, and tug. Varieties of ships were compared with one another to help inform categories. For example, crude oil tankers and petroleum tankers were originally grouped together, but when parsed out it was found that they had differing noise signatures and so they should be grouped separately. The noise from each vessel type was averaged into a noise signature for each octave band. Only container, cruise, porous, petroleum, and crude oil vessels were used in the final analysis as the other vessel types did not have consistent data.

To improve the accuracy of the ship signatures, the values were put through the sound propagation models which could then account for the hydrophone depth and approximate distance from the vessel. This yielded values which represent the sound emitted at the source, rather than the sound perceived at the hydrophone.

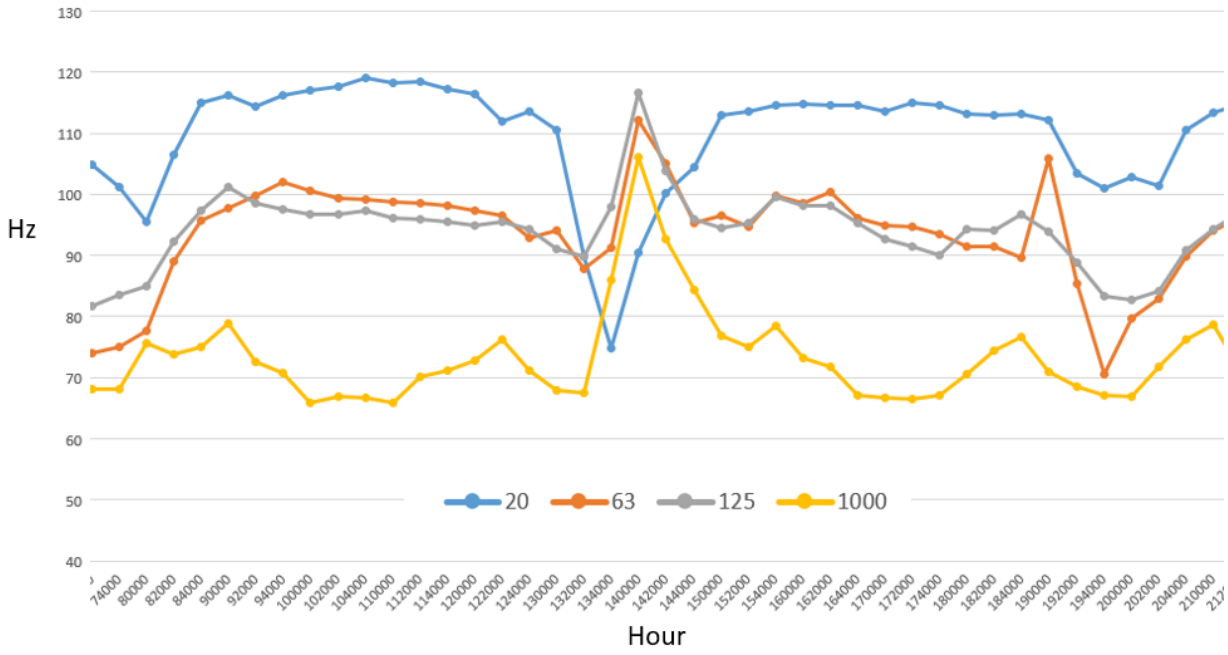

Figure 2. Excerpt from the visual analysis of the 20 (blue), 63 (orange), 125 (grey), and 1000 (yellow) ⅓ octave bands from the August 2022 hydrophone deployment adjacent to the Traffic Separation Scheme, where time is marked in hours, minutes, and seconds in 20-minute increments (i.e. 132000 = 13h20m00s) on the X-axis and the Y-axis represents Hertz starting at 40 and increasing in 10 Hz increments. The central peak (at x=140000) represents the spike in Hz when a vessel passed the hydrophone.

3.3.4. Zones of communication inhibition

Both acoustic models can provide outputs for transmission loss in four ways: transmission loss on the grid, on a specified line, pressure on the grid, and along a specified line. Transmission loss was computed using the highest pressure level on the grid as a reference. Low, medium and high inhibition levels were computed from transmission loss and two specific values related to a marine mammal's hearing thresholds. The model was run multiple times for various frequencies within a bandwidth, followed by an inverse Fourier transform to retrieve signals in time and at a particular range and depth.

The noise signatures for each vessel category at three ⅓ octave bands (63, 125, 1000 Hz) were inputted into the model to obtain a graphical output of how the noise levels (dB) travel at depth and across distances. The acoustic model was only designed for frequencies up to 1600 Hz, therefore the communication inhibition was not calculated for delphinid species or the 12500 Hz ⅓ octave band.

For this project, zones of communication inhibition were modeled along the transect for which TSS site intersects with the outgoing lane of the Traffic Separation Scheme, to present a real-world example (Figure 3a, 3b). Another transect, in the Grand Manan Basin, was modeled to demonstrate the capabilities of the model in an area with varied topography (Figure 3c, 3d).

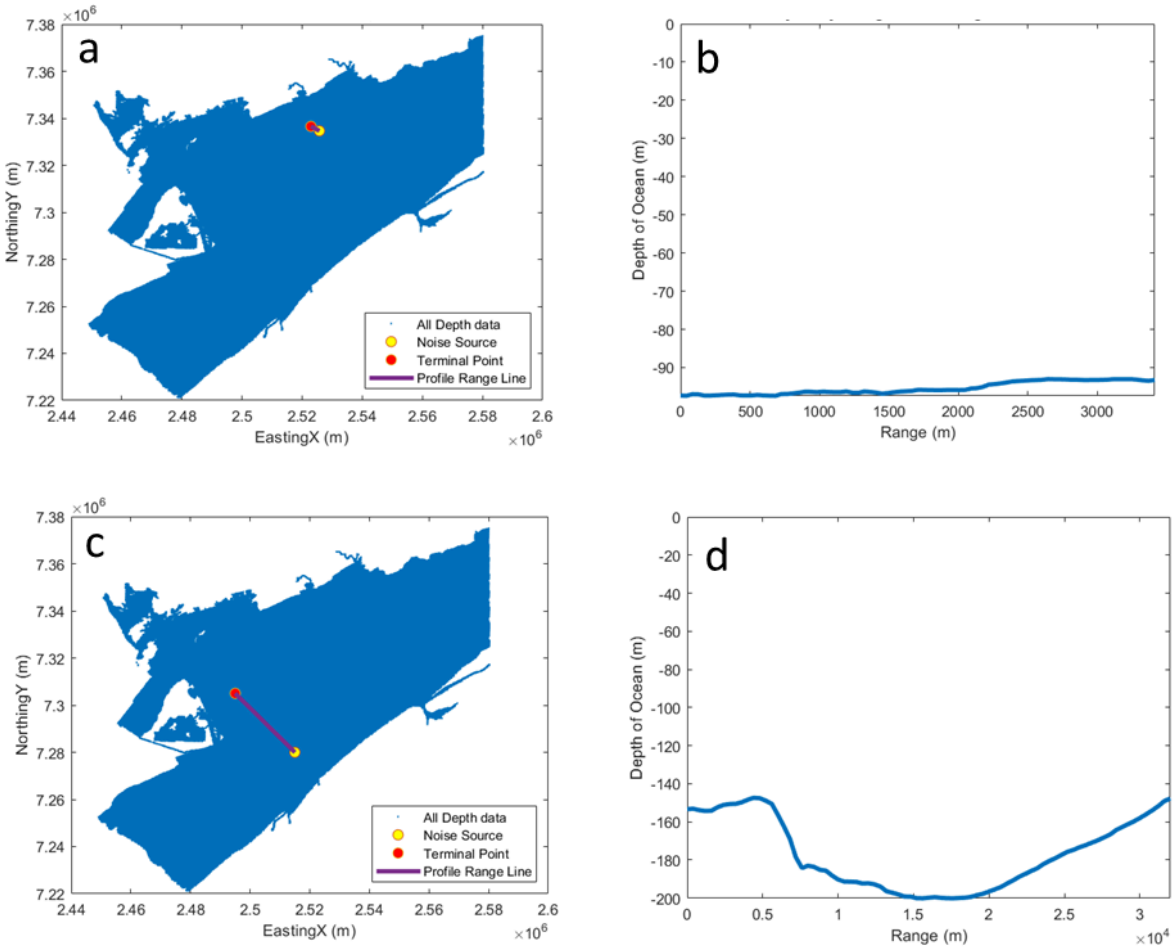

Figure 3. Model outputs of two transects in the Bay of Fundy (a, c) and their bathymetric profile (b,d); one adjacent to the outgoing lane of the Traffic Separation Scheme (a,b) and one within the Grand Manan Basin (c,d).

To accurately model the communication inhibition zones for each marine mammal species, known calling parameters (call source levels, dB re 1 µPa @ 1m) were summarized through a literature review (Appendix D). Transmission loss was calculated using the RAMSGeo model, with an approximated origin depth of 7.5 m for cruise ships and 17.5 m for all other ships. Once transmission loss for the environment was modeled and vessel signature data at a known distance from the shipping lane was obtained, it was then possible to model the noise levels through the water column for each vessel using the following equation:

Equation 3:

RL (received level, dB) = SL (source level, dB) - TL (transmission loss, dB)

Using these noise levels and a signal to noise ratio (SNR) of 10 dB, communication inhibition for each whale species was then determined for each point in range and depth. The lower bound of the low

inhibition zone was determined by the lower range of the species calling parameters, subtracted by 10. The high inhibition zone was determined by adding 10 to the upper range of the species' calling parameter range.

4.0. Results

4.1. Passive acoustic monitoring

Ten of the thirteen deployments were successful in collecting passive acoustic monitoring data (Table 2). Two equipment failures occurred (deployments 10 and 12, Table 2) which resulted in incomplete or missing data. In both instances water was found inside when the battery pack was retrieved. The pack and hydrophone were sent to OceanSonics for maintenance to prevent further loss of data. Delays to sampling were experienced throughout the 2021 season which only allowed for one deployment of the hydrophone array. An extended lobster fishing season meant deployments could not start until later in the spring to avoid tangling with fishing gear and potential loss of equipment. Meanwhile, ECW was waiting on equipment for the hydrophone array to be delivered. Finally, delays associated with contracting a vessel during the COVID-19 pandemic further prolonged the period of inactivity. However, the one deployment was a successful one, despite challenges associated with deploying over 70m of line and cable without twisting or knotting. The array collected 28 days of data. This was less than the expected 5 weeks after having converted to lithium batteries to prolong the recording time, but it should be noted that the battery pack was powering three hydrophones as opposed to one. Deployment 12 (Table 2) was unsuccessful in collecting complete data because of user error: the lines became tangled during deployment and one of the hydrophones (the middle one) was unplugged by the fishing crew without authorization from ECW staff. It was plugged back in at the wrong orientation and thus collected no data. Data from the other two hydrophones in the array were complete, though, and the bottom hydrophone on that deployment was still usable in calculating vessel signatures. A final deployment scheduled for February of 2023 was unsuccessful because of continuously inclement weather.

Passive acoustic monitoring efforts throughout this project resulted in a total of 381 days of monitoring.

Table 2. Summary of days of data recorded during project hydrophone deployments between 2019 and 2022.

Deployment	Location	Date	Days of Data
1	Grand Manan	2019.06.11	27
2	Saint John Harbour	2019.06.26	27
3	Dipper Harbour	2019.07.18	24
4	Grand Manan	2019.08.01	24
5	Dipper Harbour	2019.09.12	23
6	Grand Manan	2019.10.03	23
7	Saint John Harbour	2019.10.21	19
8	Saint John Harbour	2020.01.28	34

9	Saint John Harbour	2020.03.12	31
10	Dipper Harbour	2020.07.21	0
11	Grand Manan	2020.07.22	50
12	Grand Manan	2020.09.09	6
13	Traffic Separation Scheme	2021.10.07	28
12	Traffic Separation Scheme	2022.08.10	30
13	Traffic Separation Scheme	2022.09.13	35

4.2. Spreading loss

4.2.1. The Fundy Rose

The calculation of spreading loss (K) from the Fundy Rose ferry noise data was completed for six ⅓ octave frequency bands (63 Hz, 125 Hz, 250 Hz, 400 Hz, 500 Hz and 1000 Hz; Figure 4). However, high levels of interference (most likely from other vessels) could immediately be observed in the plots. Because of this interference masking the spreading loss relationship, the solver would only calculate a K value for three of the bands: 250Hz, K= 12.5 (Figure 4c), 400Hz, K=12.4 (Figure 4d) and 500Hz, K=14.6 (Figure 4e). Therefore, the results for the estimate of K from the Fundy Rose ferry are between 12.4 and 14.6 depending on the frequency. Figure 4a denotes the vertical shift of the curve (Y intercept).

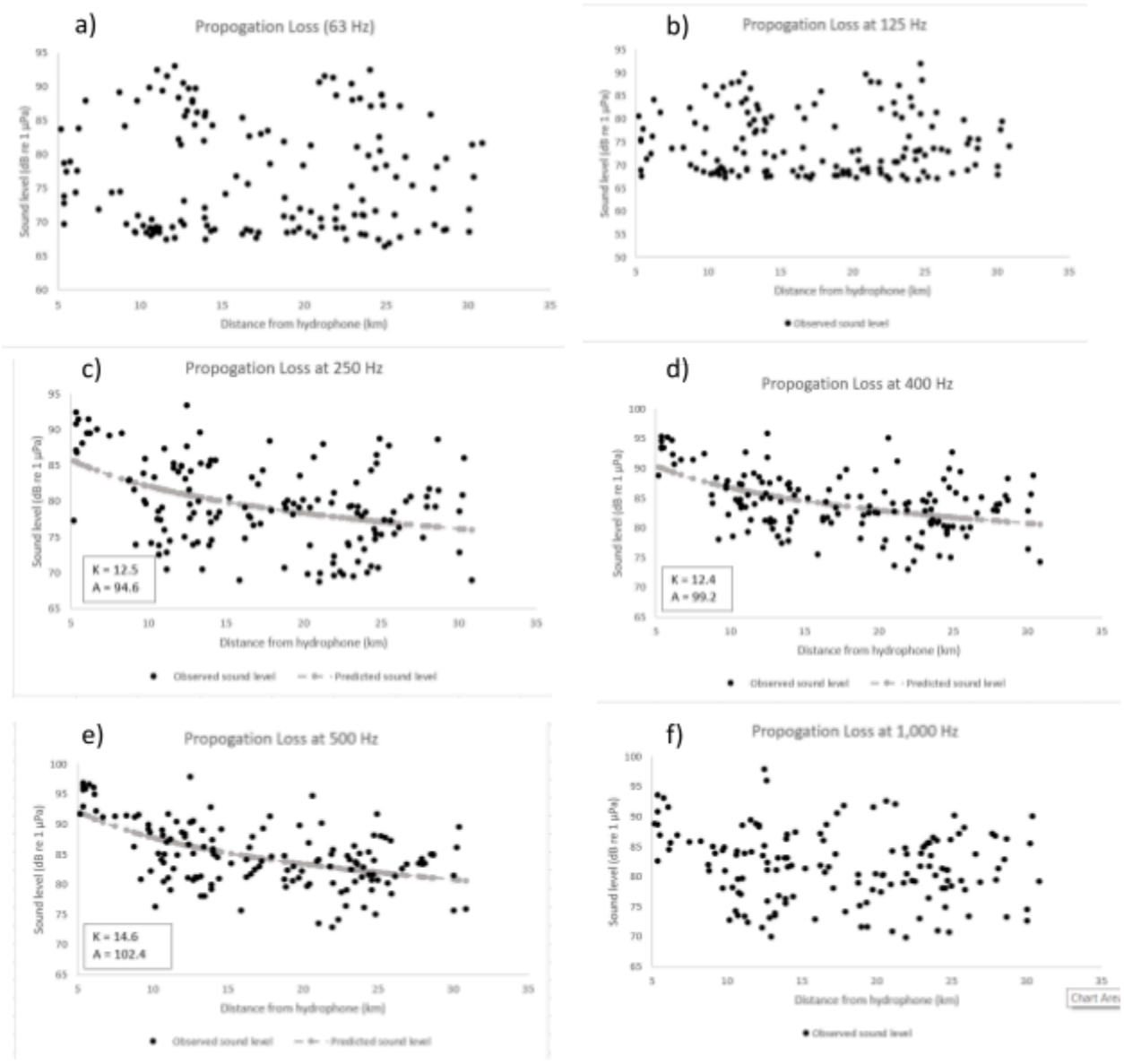

Figure 4. Solver plots for K at different bands from the Fundy Rose data, showing the amplitude (y) against the distance from the hydrophone (x) for 1/3 octave bands 63 Hz (a), 125 Hz (b), 250 Hz (c), 400 Hz (d), 500 Hz (e) and 1000 Hz (f).

4.2.2. MSC Tamara

Because of the high levels of interference masking the spreading loss relationship in the Fundy Rose analysis. An interference model was first completed (using ESRI ArcGIS) with the data for the MSC Tamara to try to identify other vessels from the surrounding area during the hydrophone active times; this allowed for selecting points which was recording during times of minimum interference (low

numbers of other vessels). This resulted in maps for two tracks for the MSC Tamara passing through the OBF, which also show the interference points of other vessels (Figure 5). The first track shows the MSC Tamara leaving the Port of Saint John on the 19th of July 2019 and passing the Saint John hydrophone (Figure 5 left) where the green circles show points on the MSC Tamara track with minimum interference and the red triangles show the interference that was removed for the model (264 interference points were removed). Most of the interference occurs within 8km of the Saint John hydrophone so only data from the Tamara past 8km was used to calculate K. The second track shows the MSC Tamara moving past the Grand Manan hydrophone entering the port on the 21st of August 2019, no interference from other vessels was recorded for this track.

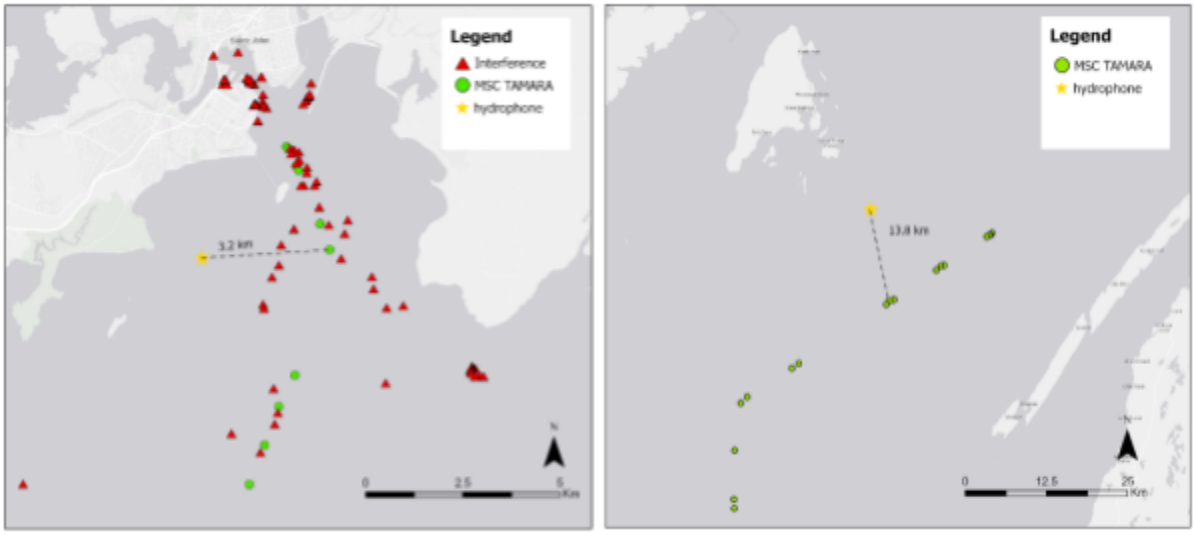

Figure 5. Maps of tracks and interference for the MSC Tamara used for the calculation of spreading loss, showing a track from the 19th of July 2019 passing the Saint John Harbour hydrophone (left) and a track from the 21st of August passing the Grand Manan hydrophone (right), ESRI ArcGIS 2020.

The results for the calculation of K based on the MSC Tamara tracks revealed no calculation of K for the 21st of August track (Grand Manan; Figure 5 right) most likely due to the vessel being too far away. The track from the 19th of July (Saint John Harbour; Figure 5 left) was usable and was used to generate solver plots for calculating K. However, only 1/3 octave bands 63Hz and 125Hz yielded any sensible results. Figure 6 shows the solver plots for calculating K for these two bands where for 63Hz, K=25.69 and for 125Hz, K=24.87. In this solver, 'A' denotes the vertical shift of the curve (Y intercept) and 'SSe' denotes the sum of squared errors and indicates comparative model fit (i.e. a lower value indicates better model fit). The results for the calculation of K from the MSC Tamara indicate that K is greater than 20.

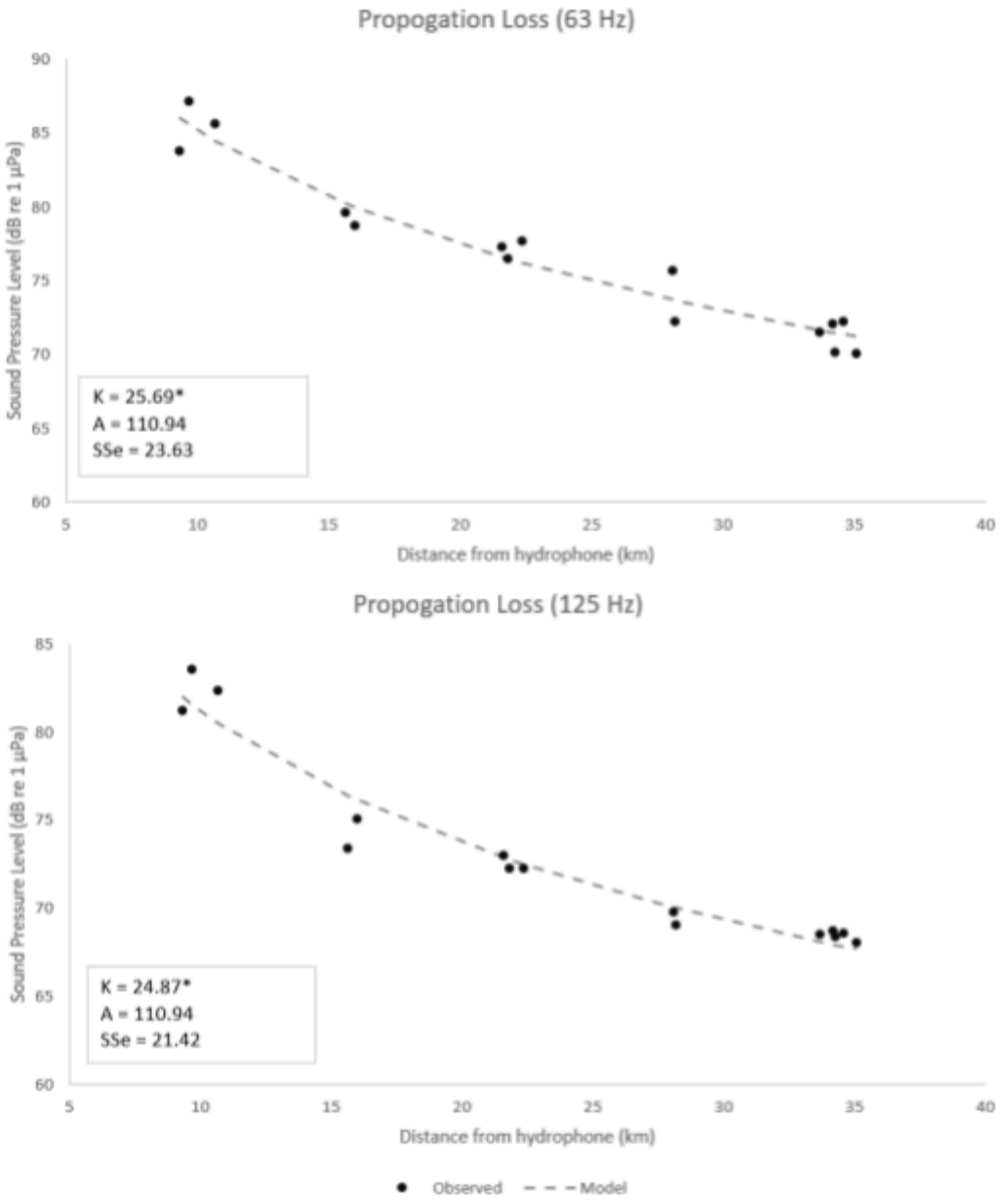

Figure 6. Solver plots for K at bands 63 Hz (top) and 125 Hz (bottom) from the MSC Tamara data from the 19th of July track around the Saint John hydrophone, showing amplitude (Y) against the distance from the hydrophone (x).

4.3. Ship signatures

A total of 189 vessels passed by the hydrophone array at the Traffic Separation Scheme site during the three deployments in 2021 and 2022, 75% of which (141 vessels) were identified and able to be used in the analysis. 26 vessels were unconfirmed because of uncertainties surrounding multiple vessels passing by the area at the same time. This may have been avoided through the purchase of AIS data, and would have brought the identification rate to 89%. 22 vessels were not detectable because of tidal strum. Of

the 141 identified vessels, 28 were container ships, 19 were cruise ships, 17 were crude oil tankers, 72 were petroleum tankers, and 5 were potash ships. Several vessels were omitted from the analysis because few to no other vessels of that class were detected and one or two vessels were not considered sufficient to represent the vessel class. These included vessels classified as: tugs (1), fish oil (1), equipment (1) and recycled metal (2).

Table 3. Noise signatures at five ⅓ octave bands for five vessel types that commonly used Port Saint John during three PAM events during 2021 and 2022; where smaller italicized numbers indicate actual recorded noise (dB) and larger bolded numbers indicate noise values (dB) adjusted for the distance and depth of the hydrophone through the use of the model. Only the 63, 125, and 1000 Hz ⅓ octave bands were adjusted for actual volume as they were the ones useful for the present analyses in the context of large marine mammal communication.

Vessel Type	20	63	125	1000	12500
Container	*107.9429*	*102.07* **160.46**	*104.1971* **156.36**	*94.81857* **131.61**	*79.22929*
Cruise	*108.2716*	*99.42789* **154.82**	*105.2063* **170.60**	*94.22895* **136.57**	*79.5*
Potash	*94.472*	*100.31* **158.70**	*107.476* **159.64**	*90.958* **127.75**	*78.198*
Petroleum	*98.46304*	*104.031* **162.42**	*108.6768* **160.84**	*97.17536* **133.97**	*82.55174*
Crude Oil	*113.5853*	*100.5167* **158.91**	*102.1227* **154.28**	*88.01867* **124.81**	*74.75867*

4.4. Modelling transmission loss and zones of inhibition

With the appropriate datasets, the models are capable of simulating underwater acoustic propagation in the outer Bay of Fundy for the purpose of studying the acoustic impact of shipping vessels to marine mammal communication. Until there is more complete seafloor data, the RAMGeo model was used because it requires fewer seafloor parameters. This comes at the expense of losing the effect of shear forces on acoustic propagation. This is explained further in the Discussion section and in full in Appendix A.

The following results were calculated based on a transect which intersected the hydrophone location and the adjacent shipping lane (Figure 3), and for environmental parameters present during the late summer and early fall.

At 125 Hz, cruise ships were the vessel type that showed the widest ranging zone of high inhibition (up to 750m away in some areas of the water column), as well as medium inhibition (up to 1500m away in

some areas of the water column) for North Atlantic Right Whales (Figure 7). Petroleum and Potash vessels showed the next largest inhibition to NARW communication: approximately 50m of high inhibition and 350m of medium inhibition (Figure 8, Figure 9). In the other NARW models, the other vessel types and frequencies had minimal inhibition and are shown in Appendix B.

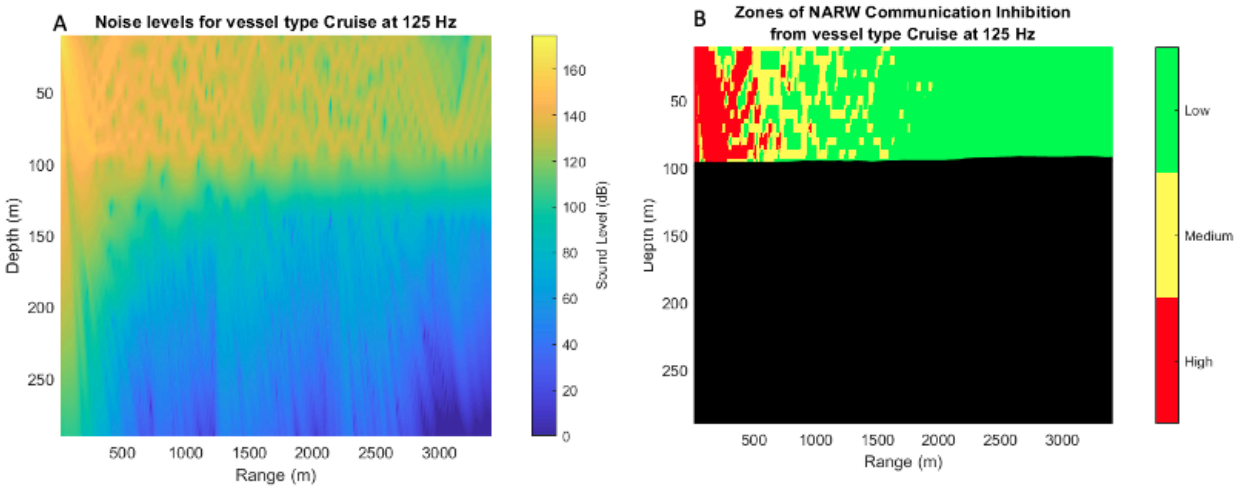

Figure 7. A) Transmission loss and associated sound levels (dB) of noise from a cruise ship class vessel at 125 Hz through the water column. B) Low, medium and high communication inhibition zones for the North Atlantic right whale (E. glacialis) from a cruise ship at 125 Hz. The calling parameters used for the NARW were 147 - 155 dB. The black portion represents the seafloor bathymetry between the noise source (vessel) and the receiver (hydrophone).

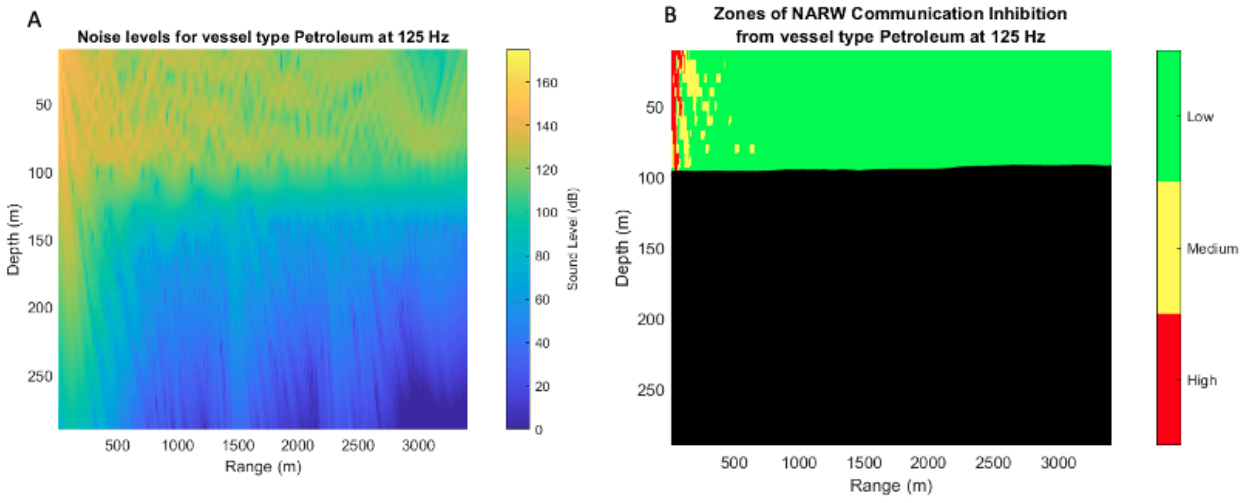

Figure 8. A) Transmission loss and associated sound levels (dB) of noise from a petroleum class vessel at 125 Hz through the water column. B) Low, medium and high communication inhibition zones for the North Atlantic right whale (E. glacialis) from petroleum vessel at 125 Hz. The calling parameters used for the NARW were 147 - 155 dB. The black portion represents the seafloor bathymetry between the noise source (vessel) and the receiver (hydrophone).

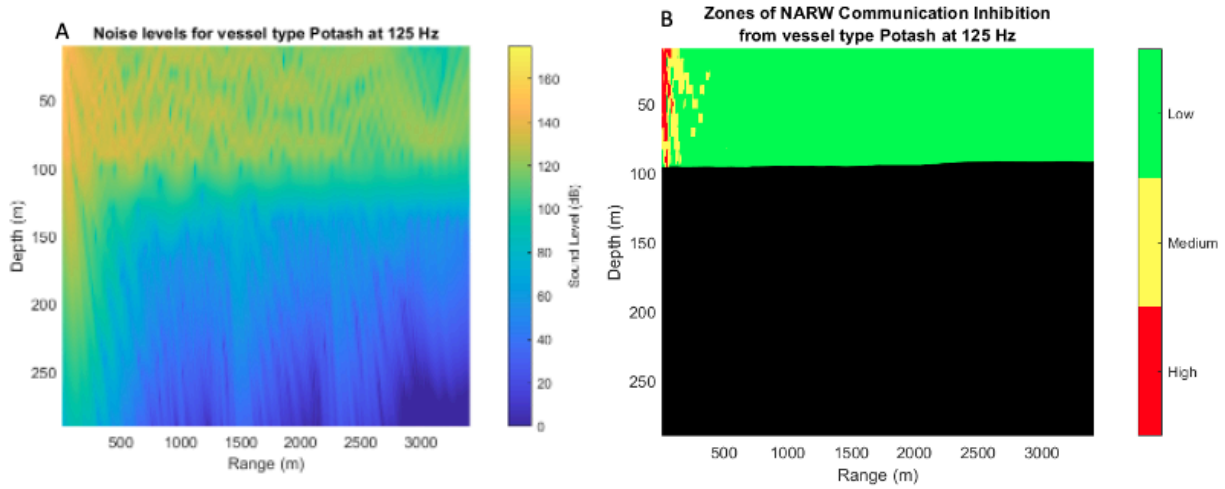

Figure 9. A) Transmission loss and associated sound levels (dB) of noise from a potash class vessel at 125 Hz through the water column. B) Low, medium and high communication inhibition zones for the North Atlantic right whale (E. glacialis) from a potash vessel at 125 Hz. The calling parameters used for the NARW were 147 - 155 dB. The black portion represents the seafloor bathymetry between the noise source (vessel) and the receiver (hydrophone).

Modelling for other species showed very minimal zones of inhibition except for humpback whales (*Megaptera novaeangliae*)(Figure 10). In the presence of a cruise ship, and at 125 Hz, the medium zone of communication inhibition extended well into the 1500m - 2000m range (Figure 10b).

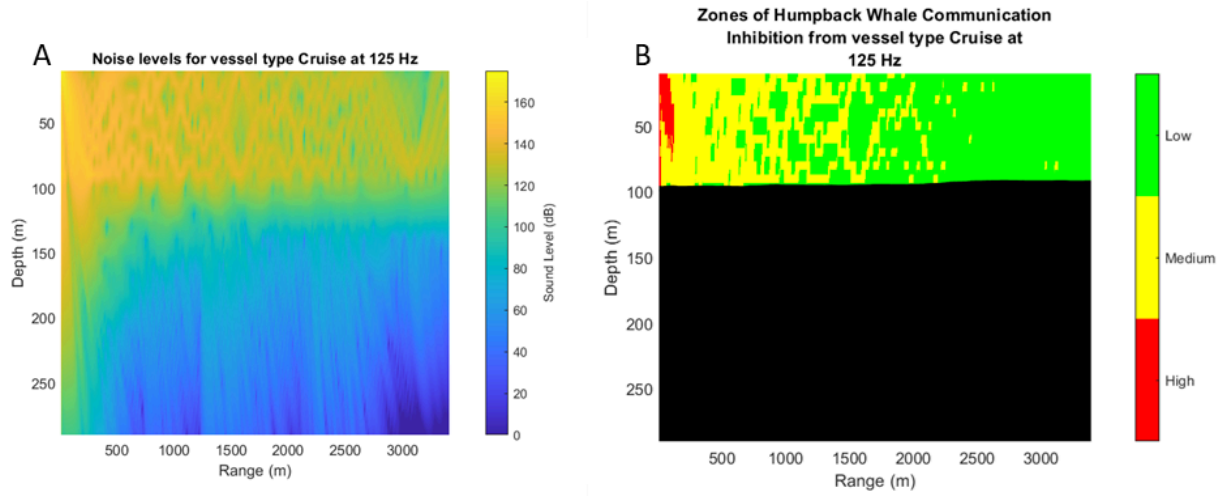

*Figure 10. Transmission loss and associated sound levels (dB) of noise from a cruise ship class vessel at 125 Hz through the water column (A); and low, medium and high communication inhibition zones for the Humpback whale (*Megaptera novaeangliae*) from a cruise ship class vessel at 125 Hz (B).*

To demonstrate the ability of the models, transmission loss and communication inhibition were also calculated for a transect in the Grand Manan Basin (see Figure 3 for transect and bathymetry profile). For a Humpback whale in the presence of a cruise ship, in the Grand Manan Basin, and at 125 Hz, the range of inhibition can be seen to extend beyond and below a ridge (Figure 11b).

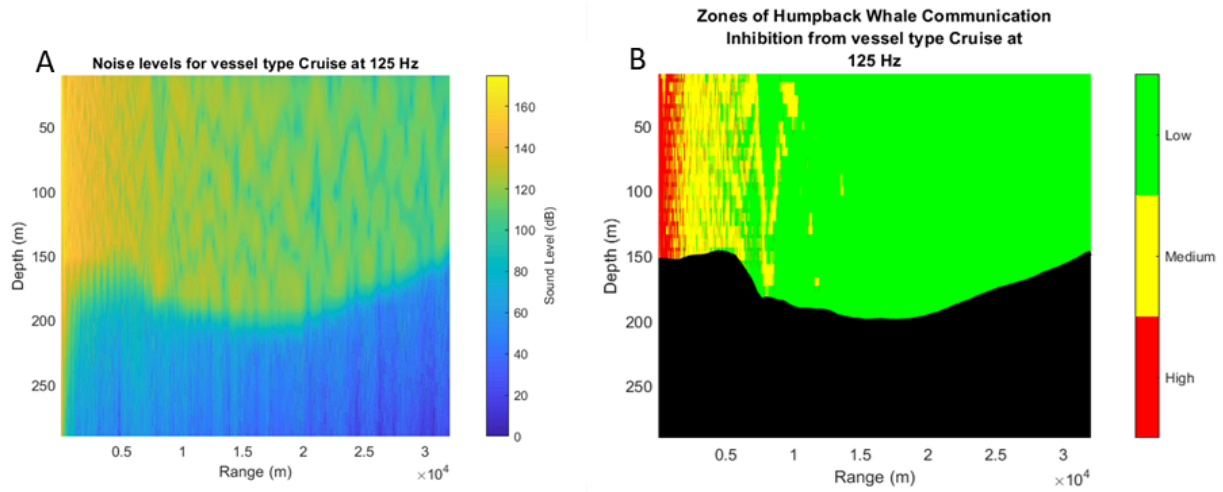

*Figure 11. Transmission loss and associated sound levels (dB) of noise from a cruise ship class vessel at 125 Hz through the water column (A); and low, medium and high communication inhibition zones for the Humpback whale (*Megaptera novaeangliae*) from a cruise ship class vessel at 125 Hz (B).*

Additional graphical model outputs for North Atlantic Right Whales (NARW) and Humpback whales are included in Appendix B. Not all figures are appended for Fin whales and Minke whales as some outputs showed nearly entirely 'low' communication inhibition.

4.5. Soundscape results and marine mammal presence

Table 4. Average ambient sound pressure levels (SPL rms) for each deployment at the traffic separation scheme used in the calculations for the vessel signatures, calculated from the average broadband sound pressure levels for every one minute of recording time.

Recording Period	Average SPL (dB re 1 µPa s)
7 Oct to 3 Nov 2021	123.7367121
10 Aug to 8 Sep 2022	122.6484344
13 Sep to 17 Oct 2022	116.2811973

The acoustic data from the collective hydrophone deployments from various projects were analyzed for marine mammal presence on a temporal and spatial scale within the outer Bay of Fundy. In depth results and analyses will be presented in a separate final report (March 2024), however, summary results are described here.

In total, five sites (Dipper Harbour, Port Saint John, Southern Wolves, Grand Manan and adjacent to the traffic separation scheme) were monitored throughout various times of the year. A minimum of nine different marine mammal species were recorded: harbour seal, grey seal, harbour porpoise, dolphin species (cannot distinguish between species), humpback, fin, minke, sei and North Atlantic right whale. Harbour seals roars were heard at all four coastal sites from May to July, and only a small number of grey seal vocalizations were heard at Port Saint John during the winter months. Sampling for harbour porpoises was done at Saint John and Dipper Harbour during April and May and were detected in high numbers during those monitoring periods. The majority of the dolphin detections were at Grand Manan and were heard from June to November, with similar results at Dipper Harbour. Dolphins were also detected at Port Saint John during the winter and spring. Fall monitoring at the traffic separation scheme also yielded dolphin detections. Humpbacks were detected at all five sites at all times of the year in high numbers. Fin whales were predominantly detected in the late summer and fall at all five sites, and had high numbers of detections during winter monitoring at Saint John. Minke whales were only heard at the TSS site August through October, despite frequenting the other sites during the summer months based on sightings records. Finally, North Atlantic right whales were detected at all sites except for Saint John, with the majority of the detections occurring in the fall (Sept/Oct).

5.0. Discussion

5.1. A working model for spreading loss in the outer Bay of Fundy

The objective to create a predictive model based on established ship signatures and anticipated scheduling to allow Port Saint John to effectively manage their underwater noise impact was partially completed through this project. The expected result was a working model that uses collected data on ship recordings and spreading loss to calculate, in real-time, amount of underwater noise in and around Saint John Harbour. To model sound propagation through these models, the user must input the amplitude, frequency, and depth of a source noise along a specified transect and at a specified time of year; to overlay zones of communication inhibition, the user must determine a range of amplitudes in a specified frequency for which a specified species of marine mammal would communicate. So, the models designed through this project do allow input of ship signatures (established through this project), while accounting for spreading loss (also established through this project) to calculate the resulting propagation of underwater noise, but they do not do so in real-time, and they do not do so for an entire port or harbour at once. Several limitations of the models prohibit those functions: namely their lack of ability to accommodate more than one source of sound at a time, their limitation to modelling along a transect, and the technical barrier that comes with the platform in which they were built. As they are unable to model multiple vessels (sound sources) at once, the models cannot practically be used in a port or busy wharf scenario. Model outputs are linear, not radial, and since the sound propagation is affected by bottom topography, many transects would be required to get an accurate picture of noise surrounding a vessel rather than in one direction away from it. The models will not run multiple scenarios / transects at once, so a user would need to run the model multiple times over to fully understand a vessel's area of impact. The model is also not very user-friendly, requiring the user to be proficient in MatLab. Next steps would require development into a web application which could be used

by managers and decision makers when they are organizing vessel traffic in busy areas, and more complex modelling to add features for practical functionality.

In addition to the practical aspects, limitations to the internal components of the models should also be considered. The following is a brief summary of the discussion points surrounding modelling spreading loss in the outer Bay of Fundy. The full details of this discussion written by the modeller, Robert White, can be found in Appendix A.

> With the appropriate datasets, the two models appear to be capable of simulating underwater acoustic propagation in the outer Bay of Fundy for the purposes of studying the acoustic impact of shipping vessels to marine mammal communication. To accurately model shipping and whale noise in the outer Bay of Fundy additional environmental data is required as well as an increased understanding of the frequencies and depths at which ships and marine mammals produce noise.
>
> The seafloor layers' compressive sound speeds, shear sound speeds, densities, compressive attenuations, and shear attenuations for the outer Bay of Fundy are the final datasets needed to get a full accurate picture of the outer Bay of Fundy environment. The seafloor layer parameter values used in the simulations are extremely rough approximations based on findings in various research papers and online sources not specific to the outer Bay of Fundy. The uppermost layer of the seafloor was assumed to have the shear and compressive sound speeds of wet sand. Given that the model does not have the actual seafloor parameters it is important to understand how the model responds to the different estimates. It is also important to know how altering the shear forces, the only substantial difference between RAMSGeo and RAMGeo, affects acoustic propagation. Lowering the shear sound speed caused the medium zones of inhibition to propagate further in range and made the RAMSGeo simulation of seawater acoustic dynamics further resemble those of the RAMGeo simulation. These estimated seafloor parameters are most likely the largest source of controllable error in this modelling project. Until there is a completed dataset, it is perhaps best to use RAMGeo because it requires less seafloor parameters, though this comes at the expense of losing the effect of shear forces on acoustic propagation.

An unexpected feature of the models was their ability to account for a source of noise at any depth or distance from a source. This will prove useful in many practical applications, for example if there were ever a need to model sound propagation from machinery at depth. In practice, this feature allowed the ship signatures calculated through this project to be adjusted (increased) since the sound received at the hydrophone, at 80 m depth and 80 m distance away from the source, would be lower than the sound emitted at the source. For this project, this adjustment was completed for each category of vessel and not each vessel's individual signature, but the same could be done for each vessel individually.

Aside from the model limitations, the accuracy of the inhibition zone outputs are limited by the available data on marine mammal communication. For the present analysis, a brief literature review was done to obtain a range of source calling levels (Appendix D) at which each species communicates for each analyzed frequency. This is by no means extensive enough to accurately represent the source level range of the species in the Bay of Fundy; it acts only as a rough estimate. Especially considering that a signal-to-noise ratio of 10dB was used since it's a commonly used value, but it is not necessarily the way

marine mammal hearing is able to process or overcome background noise to hear and discern a vocalization from a conspecific. Additionally, literature on the values for calling levels are not broken down into frequency components, rather an overall amplitude for the vocalization. Many baleen whale vocalizations contain harmonics that range in frequency and amplitude, and noise from a vessel may mask the harmonic components of the call, but not the peak amplitude. Though available known values were used to create communication ranges for the analyzed species, our understanding of baleen whale communication and hearing is limited and ultimately more extensive research is required to input absolute values into the models to obtain more accurate communication inhibition zones.

Despite these limitations, the model can serve as a good foundation for understanding how noise may affect communication space loss in baleen whales in the Bay of Fundy. Outputs here serve to demonstrate the capability of the model. The more refined the user's ability to estimate the inputs (amplitude, frequency, and depth of the source level, and communication ranges for marine mammal species at different frequencies), the more accurate the outputs will be.

5.2. Soundscape details for the Bay of Fundy

The objective to establish underwater acoustic signatures for vessels commonly passing in and out of the Saint John Harbour was completed through the resulting catalog of vessel signatures. Though it was most useful for this project to organize the ship signatures into classes of vessel (cruise ship, container ship, petroleum ship, container ship), the project outputs include a dataset of all analyzed vessels (Appendix C). Smaller vessels and ferries were not analyzed through this project as the port departure schedule was used to identify passing vessels rather than AIS. If required in a noise management context, ferry noise could be analyzed through the passive acoustic monitoring data collected in the first stages of this project, or through some of ECW's past monitoring. A major accomplishment through this project was the spreading loss calculations which are unique to this region, which could be useful in other projects going forward.

The vessel signatures calculated through this project contain two primary limitations: the position of the vessels with respect to the hydrophone, and the accuracy of the calculated vessel signatures. Complete vessel compliance with the traffic separation scheme is unlikely given navigation can change based on sea and weather conditions, meaning vessels may have may not have been in the exact center of the outgoing shipping lane while passing by the hydrophone site. Since the models were used to correct the amplitude of the vessel at the surface based on their anticipated distance from the hydrophone, the estimates could be slightly skewed if the vessel was closer or further from the hydrophone. Further, even if the vessels did all travel past the hydrophone in the expected position, some vessels which left the port during the deployment periods were not detected by the hydrophone over the interference that the tides were creating as waterborne particles passed over the unit. As a result of the interference, it's possible that the vessel estimates are slightly higher than they should be as the quieter vessels could not be included in the calculations through these methods. As the percentage is small relative to the dataset available, it's unlikely that the signatures would change drastically. Another aspect of the analysis which might factor into the accuracy of the vessel signatures include the fact that some vessel classes had relatively small numbers. To improve the vessel signatures calculated here, further monitoring could take place in a location with less flow to reduce the interference caused by the tide. In contrast, it's also possible that the estimates are slightly lower than they should be for some vessels which may have been

passing the hydrophone at a time between recording periods. The hydrophone records 5 out of every 20 minutes, meaning that there is 15 minutes between recordings. Throughout the visual assessment, several vessels showed two distinct peaks in different octave bands at different times (consecutive recordings). For example, a vessel's amplitude may have peaked at the 125 Hz ⅓ octave band peaked at 19:00 with a value of 102.28 Hz, and the 63 Hz ⅓ octave band may have peaked at 19:20 with a value of 108.47 Hz. It is unclear whether this is a result of the vessel passing by in between the recording periods or whether the sound is propagating differently at different octave bands. The proportion of vessels for which this was the case was not calculated during the analysis, though it was certainly a small minority. In the future, it would be useful to ground truth model outputs.

Communication inhibition for most mammal species and ⅓ octave bands (in the presence of a singular vessel) remained relatively low compared to those inhibition figures which were included in this report. Disruption to minke and fin whale communication was also relatively minimal in all scenarios. Although not all model outputs were included in the results in this document, it is clear from the complete set of model outputs (additional figures are included in Appendix B) that cruise ships are the most disruptive to marine mammal communication overall. More specifically, cruise ships tended to show the most impact on humpbacks and NARW. Extrapolating the approximate 1000 m zone of high to medium inhibition for NARW in the presence of cruise ships at the 125 Hz ⅓ octave band into a radius, this would indicate the potential to send and/or receive communications within one kilometer of the vessel in any direction. If the model functions were to be improved to demonstrate the compounding between two vessels, it would be important to then understand the interaction between multiple cruise ships at the same time, potentially drastically increasing that radius. This is especially important given that many cruise ships visit the port in the course of a year, and may exist in the same space at multiple points along their route to and from Port Saint John, which passes through NARW critical habitat in the Grand Manan Basin. It is also important in the context of the space in which NARW are occupying more frequently in the Bay of Fundy outside of the critical habitat: the area between the West Fundy Isles, the Wolves Islands, and Campobello, which has seen increasing cruise ships in recent years commuting from Eastport, Maine through the isles and up to Port Saint John, according to some researchers in the area.

Spatiotemporal information about marine mammal calls recorded through the passive acoustic monitoring during this project was an expected result, but it was found that this was more resource-intensive than originally anticipated. This work is currently underway through a separate project, and is occurring for all of ECW's passive acoustic monitoring data from 2015-2022.

5.3. Project objectives

This project improved the understanding and capacity for management of underwater noise in the outer Bay of Fundy through multiple results. Localized information on the soundscape of the outer Bay of Fundy, including specific rates of spreading loss and the catalog of ship signatures will greatly facilitate future work on this subject. Further, the extensive research and data accumulated through this project to build the models, the models themselves, and their ability to produce useful outputs can serve to elevate the quality of noise management in our region. The state of knowledge in our region is substantially advanced by having such specific and localized information. The results from this project can be an asset to Port Saint John and potentially also to other users interested in advancing their management of auditory habitat.

The objective to establish passive acoustic monitoring locations on either side of the Bay of Fundy Traffic Separation Scheme was not completed. Originally, one was to be stationed east of White Head Island (Grand Manan) and another was to be stationed west of Digby Neck. The Grand Manan hydrophone site fulfills the former, but the latter was not established. Challenges to deployments during the COVID-19 pandemic, combined with increased costs in the materials required for establishing the hydrophone array, restricted monitoring to a single site during the second phase of the project (2021 and 2022). In this phase, a site adjacent to the Traffic Separation Scheme part way between Port Saint John and Grand Manan was established to accommodate the added considerations of deploying an ISO-compliant hydrophone array. That site was also selected because it would be more relevant for the analysis of ship signatures, which proved true. The port records incoming and outgoing vessels, but it was more consistent that outgoing vessels would leave directly and pass by the hydrophone adjacent to the outgoing lane. Incoming vessels would be more challenging to identify, especially since vessels can be required to wait outside the port before being let in. In the future, AIS ship tracking should be used to facilitate this process and eliminate a small percentage of ships that were omitted from this study. However, visual analysis of this data would still be required because some vessels were not detected at all beyond the noise interference caused by the tidal motion, especially if the vessel passed the hydrophone site during mid tide rising or mid-tide falling. It should be noted that it was suggested to ECW by staff at JASCO Applied Sciences that a vertical hydrophone array not continue to be used in the Bay of Fundy because of the amount of noise interference generated by the flow of tidal water; a horizontal array would have much more success.

5.4. Conclusions

An overarching objective in this project was to increase the understanding and capacity for management of underwater noise in the outer Bay of Fundy. This was achieved through the expected results, which were to generate a catalog of ship recordings, to create a better understanding of the details of the local soundscape, to calculate a rate of spreading loss specific to this region, and to generate a working model which combines the vessel signatures, soundscape details, and local spreading loss to understand the amount of underwater noise in the outer Bay of Fundy. Broadly, these results were achieved.

Future work should focus on bettering our understanding of marine mammal communications, and on enhancing the model to be able to work for the Port. Much of the groundwork has been completed which would allow this research to be used by the Port as a tool for management of underwater noise. With input from a web developer, this work could create an incredibly useful application which could be used in high traffic areas throughout the Bay of Fundy, not just for management of vessels traveling to and from the port.

6.0. References

Buzeta, M. I., Singh, R., and Young-Lai, S. 2008. Identification of Significant Marine and Coastal Areas in the Bay of Fundy. Fisheries and Oceans Canada. Canadian Manuscript Report of Fisheries and Aquatic Sciences. 2635. 292 p.

European Union (EU), 2008. Marine Strategy Framework Directive (MSFD).

Erbe C, Marley SA, Schoeman RP, Smith JN, Trigg LE and Embling CB. 2019. The Effects of Ship Noise on Marine Mammals—A Review. *Front. Mar. Sci.* 6:606.

DELTA. 2014. noiseLAB Capture Professional (v4.0.4). [Software]. [Date Accessed: March 2020].

International Organization for Standardization (ISO). 2016. Underwater acoustics – Quantities and procedures for description and measurement of underwater sound from ships – Part 1: Requirements for precision measurements in deep water used for comparison purposes (Standard No. 17208-1).

Lawrence, C.B. 2023. Acoustic Data Processing Report: Bay of Fundy Data Collection (2020-2022). Document 03154, Version 1.0. Technical report by JASCO Applied Sciences for Eastern Charlotte Waterways Inc.

Port Saint John, 2023. Previous Ships in Port. URL https://vessels.sjport.com/webx/#

R Core Team (2019). R: A language and environment for statistical computing. R Foundation for Statistical Computing, Vienna, Austria. URL http://wwww.R-project.org/.

Richardson, WJ., Greene CR, Malme CI., Thompson, DH. 1995. Marine mammals and noise. Academic Press, San Diego, CA.

Zhang, G., Forland, TN., Johsen, E., Pedersen, G., Dong, H. 2020. Measurements of underwater noise radiated by commercial ships at a cabled ocean observatory. *Marine Pollution Bulletin*. 153.

7.0. Appendix A: *An assessment of underwater acoustic propagation models for estimating commercial shipping noise in the outer Bay of Fundy*

The following is a report titled *An assessment of underwater acoustic propagation models for estimating commercial shipping noise in the outer Bay of Fundy* (2021) written by Robert White who was hired on a contract at ECW to complete this research.

7.1. Introduction

The underwater noises that commercial shipping vessels produce are known to interfere with marine mammal behaviour. Marine mammals are vulnerable to underwater anthropogenic noises because they rely on underwater acoustic signals for communication, navigation, and hunting. Amongst the set of marine mammals is the critically endangered North Atlantic Right Whale (NARW). The NARW, as well as active commercial shipping vessels, can be found in the Bay of Fundy during the summer months. Environmental groups, such as Eastern Charlotte Waterways (ECW), are concerned that the underwater noises produced by the shipping vessels in the outer Bay of Fundy will push the NARW ever closer towards extinction. For this reason, ECW launched their underwater noise project with the intention of monitoring and modelling the acoustic impact that commercial shipping vessels have in the outer Bay of Fundy. Hydrophones will be deployed in the outer Bay of Fundy to monitor the soundscape. The RAMGeo and RAMSGeo ocean acoustic models will be used to simulate the acoustic noise and transmission loss produced by ships in the outer Bay of Fundy. The models are useful because it is impractical to deploy hydrophone arrays across the entire outer Bay of Fundy during the entire whale season. The purpose of this report is to display the capabilities of the RAMGeo and RAMSGeo ocean acoustic models, as well as critique their performance and discuss missing data necessary for the modelling component of the project.

7.2. Methods

RAMGeo and RAMSGeo are underwater acoustic propagation models that can handle low frequencies and range dependent environments. RAMGeo treats the seafloor as a fluid whereas RAMSGeo accounts for the shear forces in the seafloor by treating it as an elastic. Three other key physical assumptions of the models are (1) the pressure and forcing term are harmonic, (2) the azimuths are uncoupled, and (3) outgoing energy dominates back scattering energy. The uncoupled azimuth approximation removes the azimuth dimension from the cylindrical coordinate system so that the only spatial dimensions being considered are range and depth, where range is the horizontal distance from the sound source in meters and depth is the depth below the ocean surface in meters. The models generate numerical solutions to the wave equation in the form of an outgoing cylindrical wave that is propagating energy at small angles to the horizontal by utilizing a split-step Padé algorithm. The models are only capable of handling one frequency at a time.

Each model requires an environment file with an env extension as the input. The environment files define the physical and numerical properties of the ocean environment along a particular azimuth from the sound source, as well as properties of the sound source. The physical parameters include the

bathymetry and sound speed profile in the ocean, as well as material properties, such as density and attenuation, of the solid layers below the seafloor. The bathymetry is computed using inverse distance interpolation with the available 250m Easting/Northing resolution outer Bay of Fundy depth data for each of the 81 equally spaced coordinates along the straight line defined by the sound source coordinate and a terminal coordinate. Sound speed profiles are calculated using the GSW MATLAB library with thermodynamic data from the outer Bay of Fundy and averaged at different depth slices for each month. The densities and attenuations of the solid sub-surface layers were estimated from research papers [1,4,5]. The compressive and shear sound speeds of the solid sub-surface layers were roughly estimated from a variety of online sources [2,3]. The two acoustic source parameters are the frequency of the sound source in Hertz and the depth of the sound source in metres. Numerical parameters are tuned for convergence and spatial resolution purposes.

The models output the files tl.grid, tl.line, p.grid and p.line which are the transmission loss on the grid, transmission loss along the specified line, pressure on the grid and pressure along the specified line, respectively. The grid is composed of a set of range and depth coordinates defined by numerical parameters in the input files.

All the ocean, acoustic and numerical information are written to an environment file in MATLAB. The environment file is copied into a ramsgeo.in or ramgeo.in file so that it can be recognized by the acoustic model of choice. The acoustic model of choice is executed via the command line and the pressure grid is read into MATLAB using the readrampgrid function in the CMST Software package (actup). Transmission loss is computed with the maximum value on the pressure grid as the reference pressure. Three zones of inhibition level to marine mammal communication, high, medium, and low, are computed from Transmission Loss and two marine mammal transmission loss hearing threshold values. For a bandwidth of frequencies, the model is run multiple times for each frequency in the discretized bandwidth and then an inverse Fourier transform is applied to retrieve signals in time at a particular range and depth. The time signal is assumed to be purely real and conjugate symmetry is utilized to extract information regarding the negative frequencies for the inverse Fourier transform. Tables 1 and 2 describe the four simulations that were run to display the performance of the models as well as our capabilities with the model output. Figure 1 is a reference map of the whale sighting zone and shipping lanes in the outer Bay of Fundy. Sound source and terminal coordinates are in the outer Bay of Fundy and in the New Brunswick Stereographic projection (NBDS).

Table 1: Coordinates, model version and month for each simulation. The coordinates are with respect to the (NBDS) projection. Sound Sources are chosen along the incoming and outgoing shipping vessels in the outer Bay of Fundy.

Simulation #	Sound Source Coordinate		Terminal Coordinate		Version	Month
	Easting (m)	Northing (m)	Easting (m)	Northing (m)		
1	2514845.613	7291599.161	2511303.41	7288529.208	Rams	8
2	2514845.613	7291599.161	2511303.41	7288529.208	Ram	8
3	2520728.372	7286449.966	2513919.131	7287707.936	Rams	8
4	2520728.372	7286449.966	2513919.131	7287707.936	Ram	8

Table 2: Acoustic source and receiver information for each simulation.

Simulation #	Source Frequency/Bandwidth (Hz)	Source Depth (m)	Frequency Resolution (Hz)	Receiver Range (m)	Receiver Depth (m)
1	125	10	N/A	N/A	N/A
2	125	10	N/A	N/A	N/A
3	[112,141]	10	1	100	40
4	[112,141]	10	1	100	40

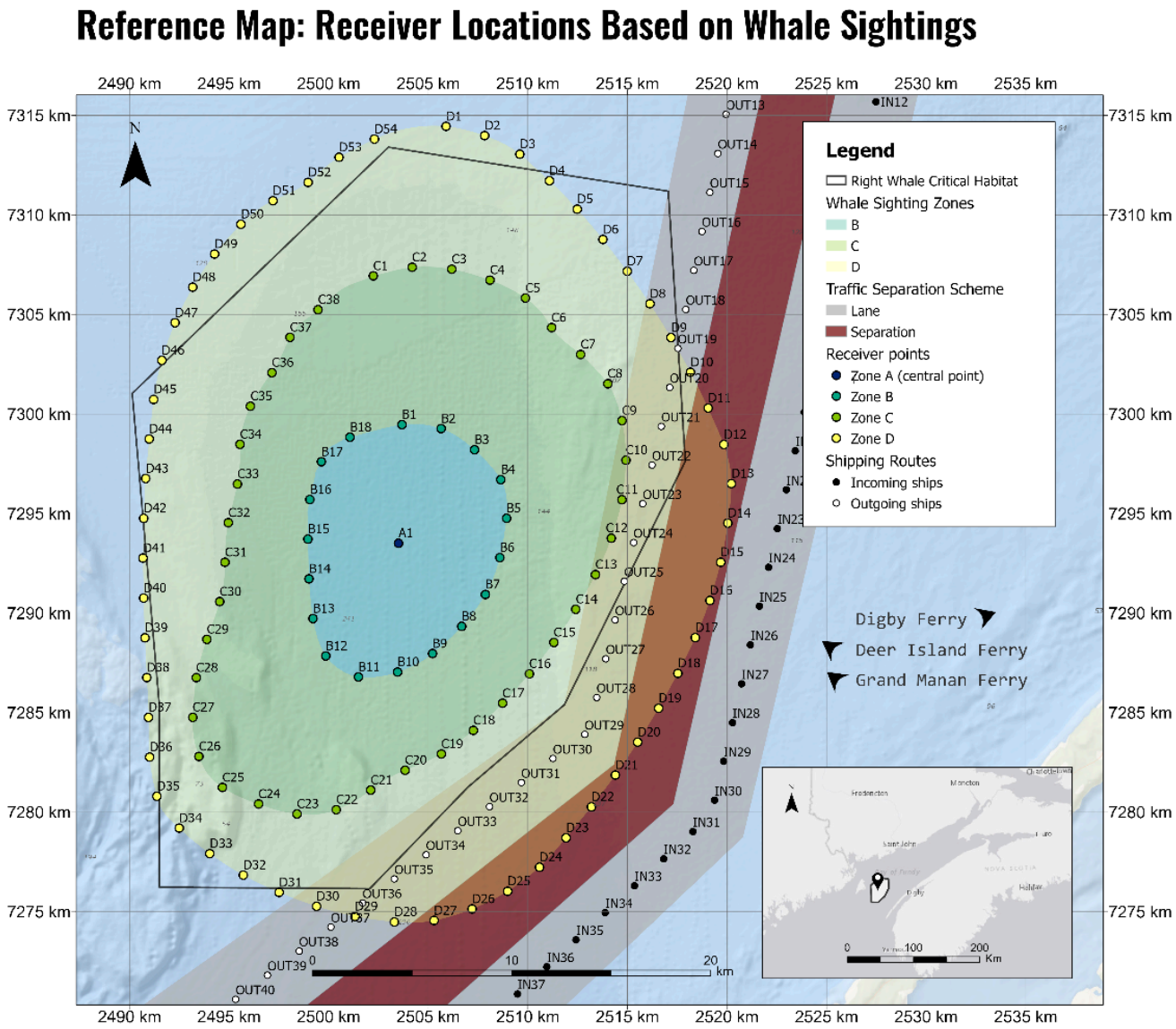

Figure 1: Reference map displaying the outgoing and incoming shipping lanes in the outer Bay of Fundy as well as the whale sighting zone. The horizontal axis is Easting, and the vertical axis is northing (NBDS). Outgoing (Incoming) ships travel along the grey lane just west (East) of the red separation line. The circular regions colored green, yellow and blue are regions of the whale sighting zone.

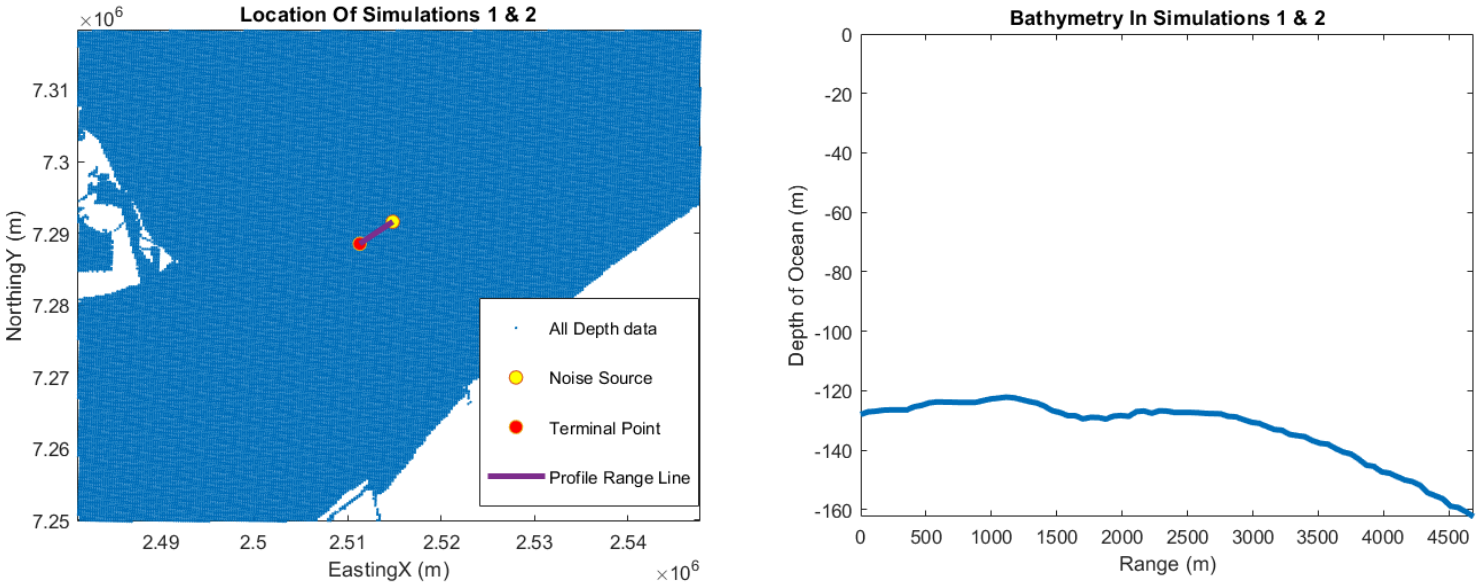

(a) *(b)*

Figure 2: Location (a) and bathymetry (b) of simulations 1 and 2 described in table 1. The coordinates in (a) are with respect to NBDS. 0m depth in (b) is the ocean surface and negative depths are below the surface (underwater), the blue line in (b) traces out the ocean depth along the profile range line in (a) with 0m range being the sound source and the largest recorded range value being the terminal point. In these simulations the profile range line is roughly 4.5km.

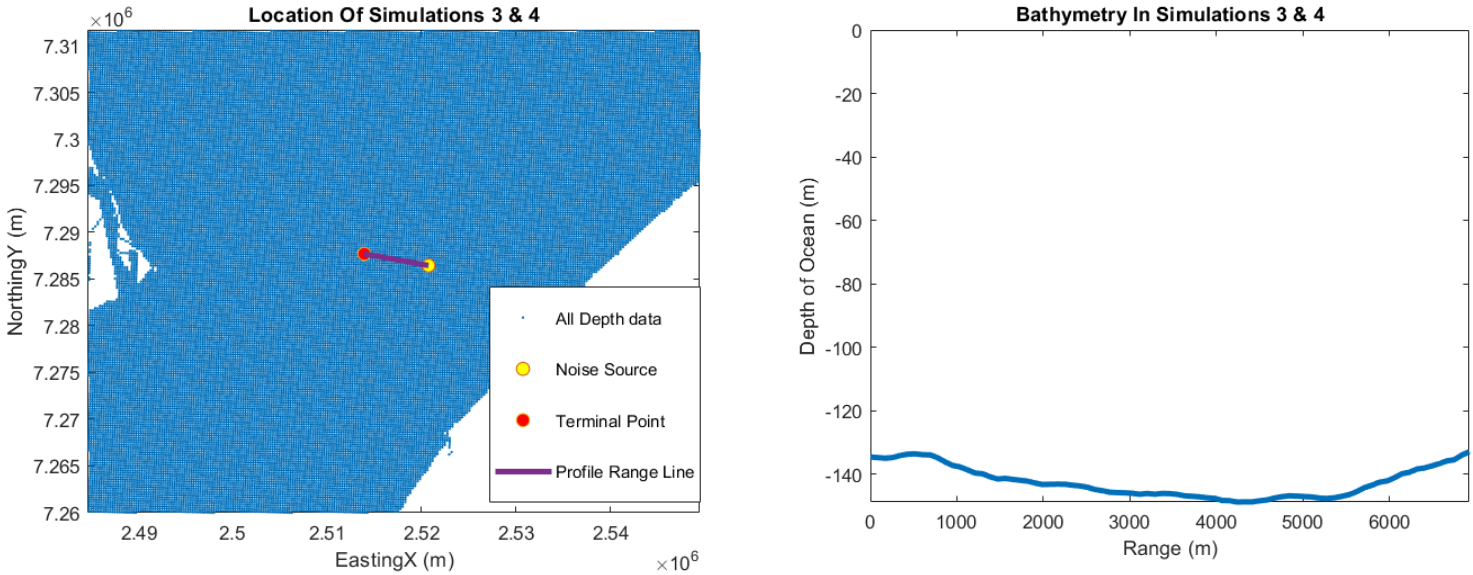

(a) *(b)*

Figure 3: Location (a) and bathymetry (b) of simulations 3 and 4 described in table 1. The coordinates in (a) are with respect to NBDS. 0m depth in (b) is the ocean surface and negative depths are below the surface (underwater), the blue line in (b) traces out the ocean depth along the profile range line in (a) with 0m range being the sound source and the largest recorded range value being the terminal point. In these simulations the profile range line is roughly 7.0km.

7.3. Results

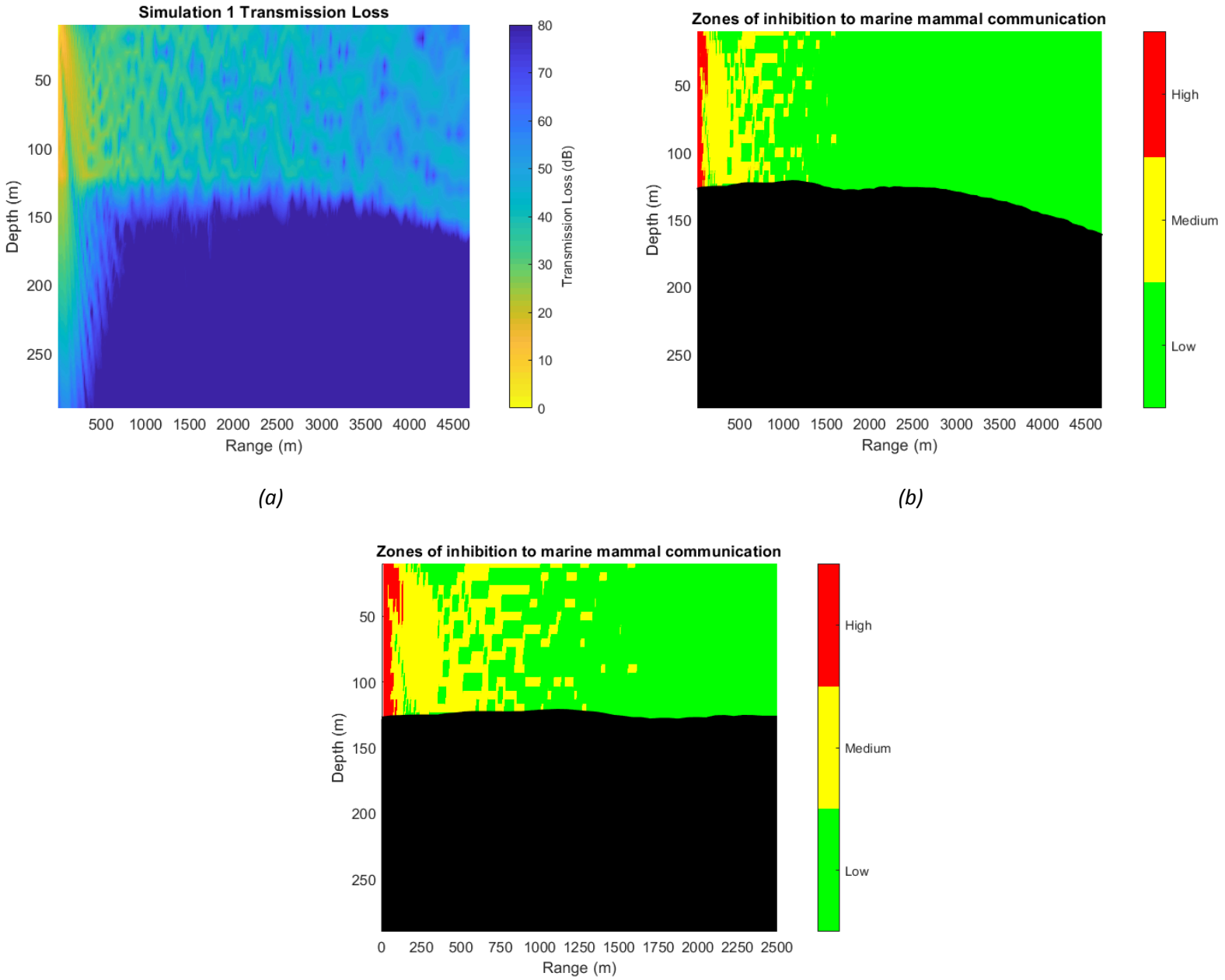

Figure 4: Transmission loss (a) and zones of inhibition to marine mammal communication (b) for simulation 1. (c) is a rescaled version of (b). The zones chosen for (b) and (c) are acquired from (a) by [0,17]TL – High, (17,33]TL – Medium and (33,+)TL – Low. The black portion in (b) and (c) is the seafloor. 0m depth is the ocean surface and positive depth is below the ocean surface (underwater).

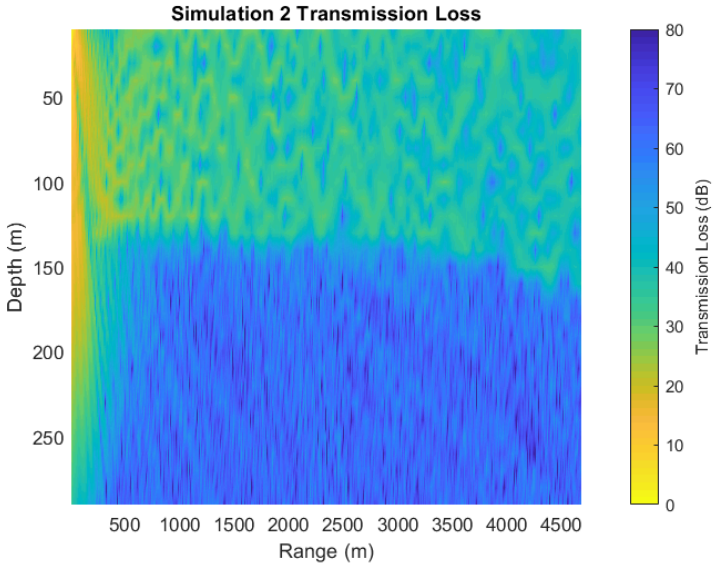

(a)

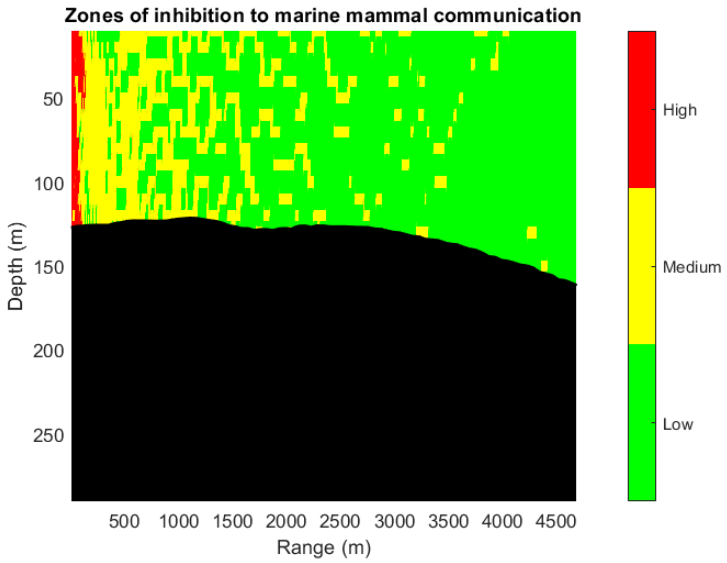

(b)

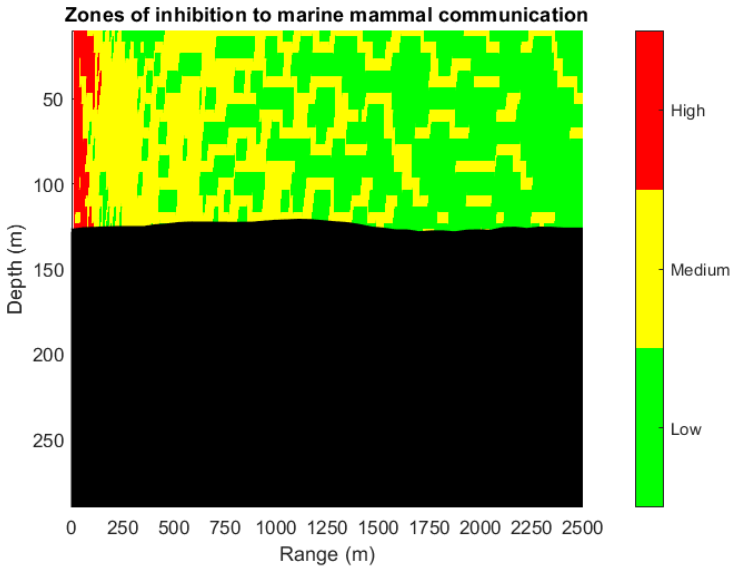

(c)

Figure 5: Transmission loss (a) and zones of inhibition to marine mammal communication (b) for simulation 2. (c) is a rescaled version of (b). The zones chosen for (b) and (c) are acquired from (a) by [0,17]TL – High, (17,33]TL – Medium and (33,+)TL – Low. The black portion in (b) and (c) is the seafloor. 0m depth is the ocean surface and positive depth is below the ocean surface (underwater).

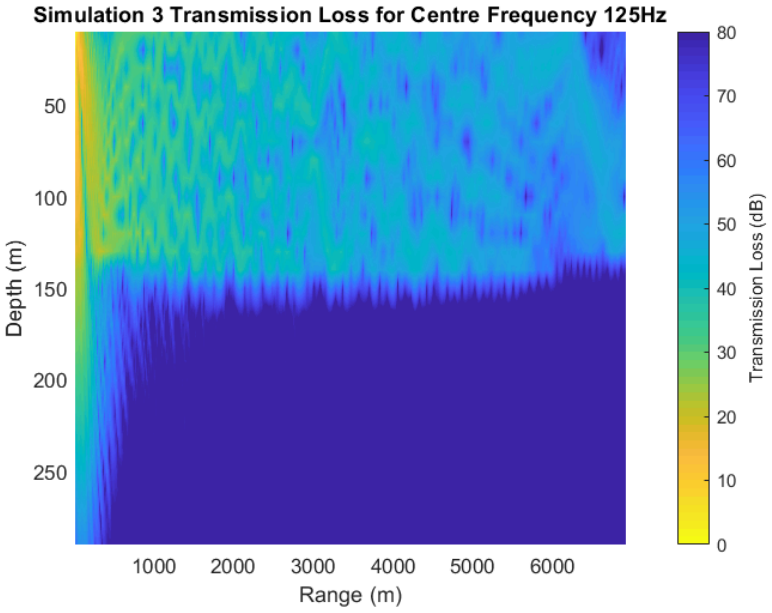

(a)

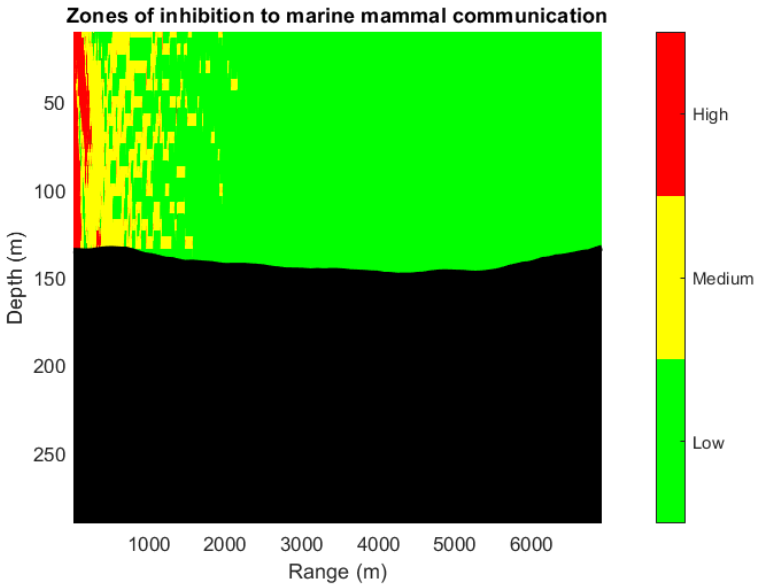

(b)

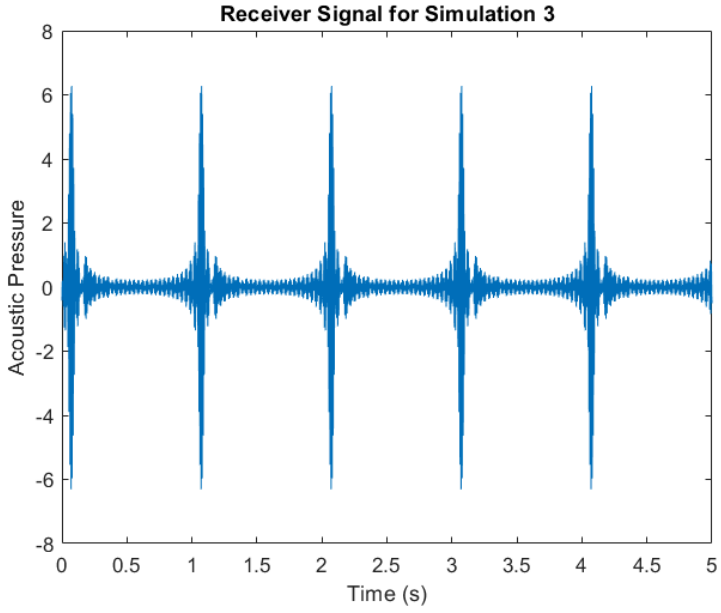

(c)

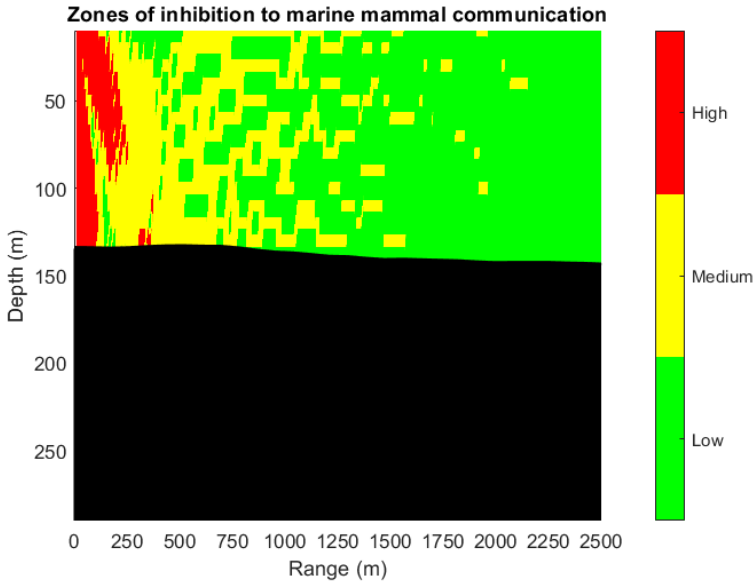

(d)

Figure 6: Transmission Loss for centre frequency 125Hz (a), zones of inhibition to marine mammal communication (b), and computed signal at receiver (c) for simulation 3. (d) is a rescaled version of (b). The zones chosen for (b) and (d) are acquired from (a) by [0,22]TL – High, (22,35]TL – Medium and (35,+)TL – Low. The black portion in (b) and (d) is the seafloor. 0m depth is the ocean surface and positive depth is below the ocean surface (underwater). Refer to table 2 simulation 3 for more information regarding the constructed signal (c).

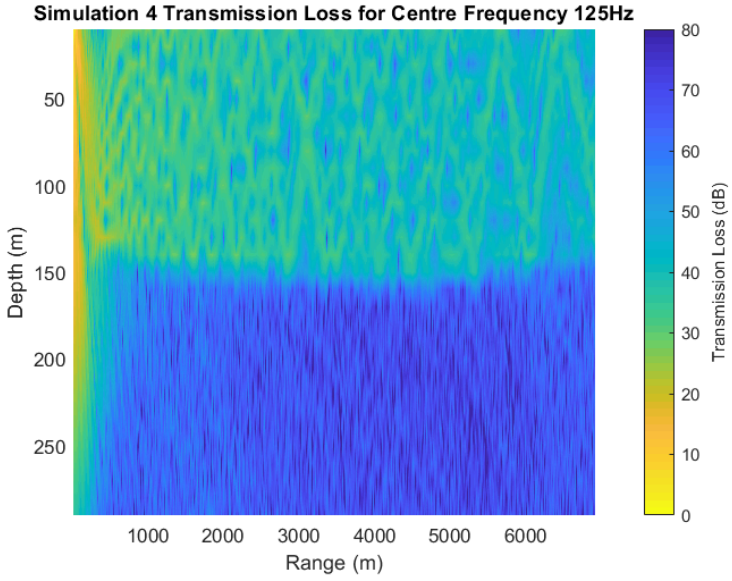

(a)

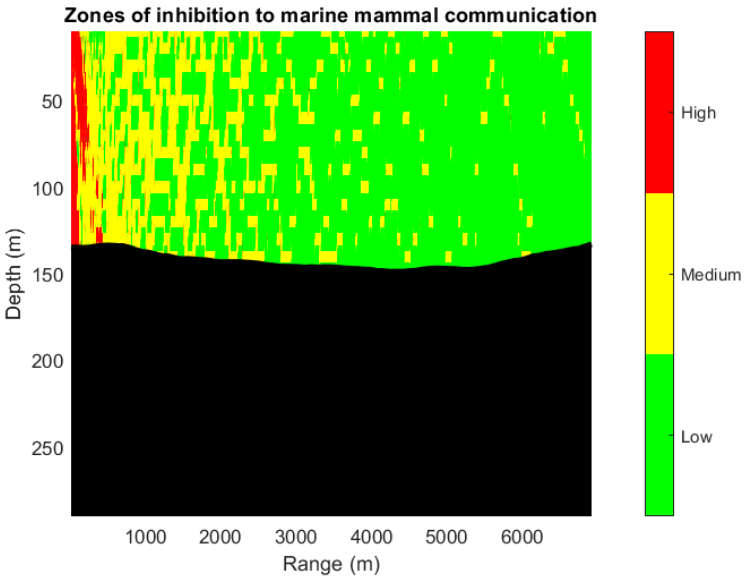

(b)

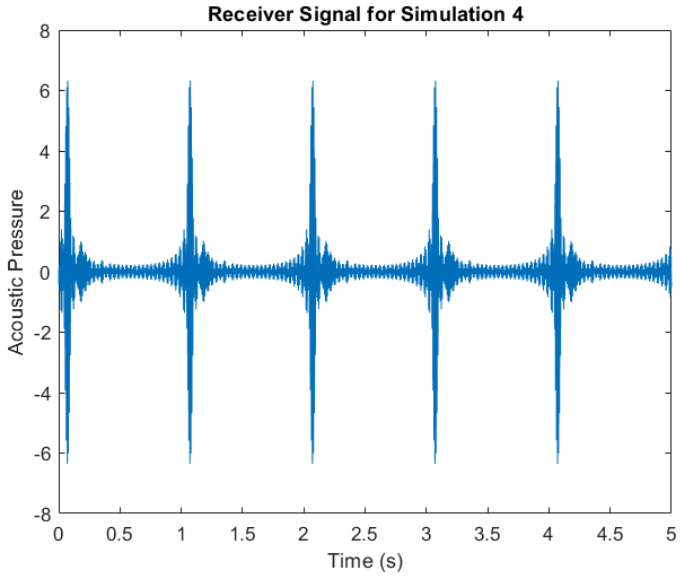

(c)

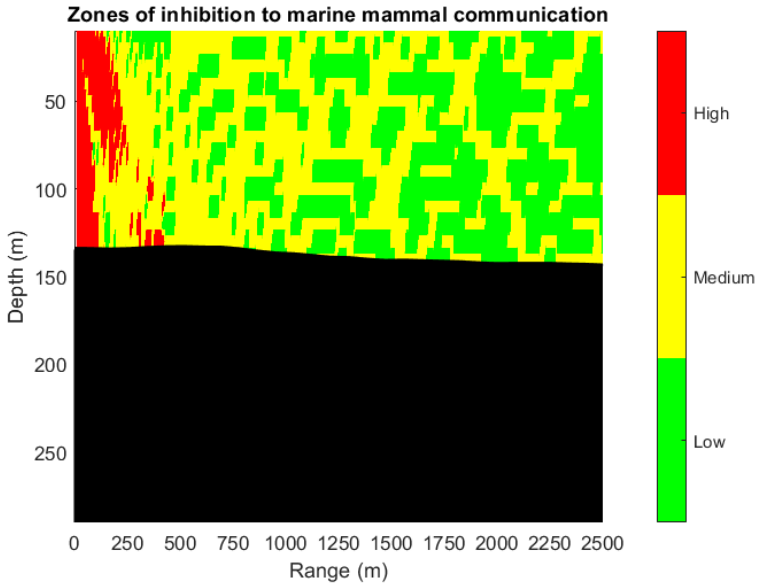

(d)

Figure 7: Transmission Loss for centre frequency 125Hz (a), zones of inhibition to marine mammal communication (b), and computed signal at receiver (c) for simulation 4. (d) is a rescaled version of (b). The zones chosen for (b) and (d) are acquired from (a) by [0,22]TL – High, (22,35]TL – Medium and (35,+)TL – Low. The black portion in (b) and (d) is the seafloor. 0m depth is the ocean surface and positive depth is below the ocean surface (underwater). Refer to table 2 simulation 4 for more information regarding the constructed signal (c).

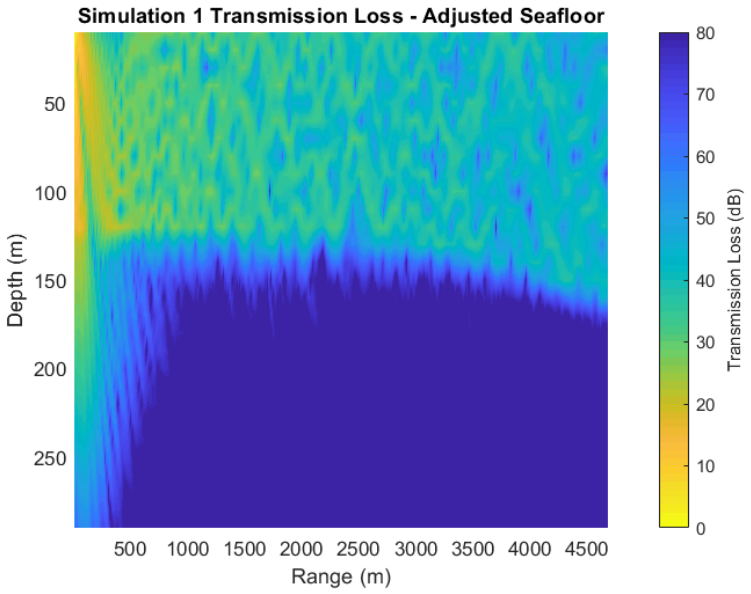

(a)

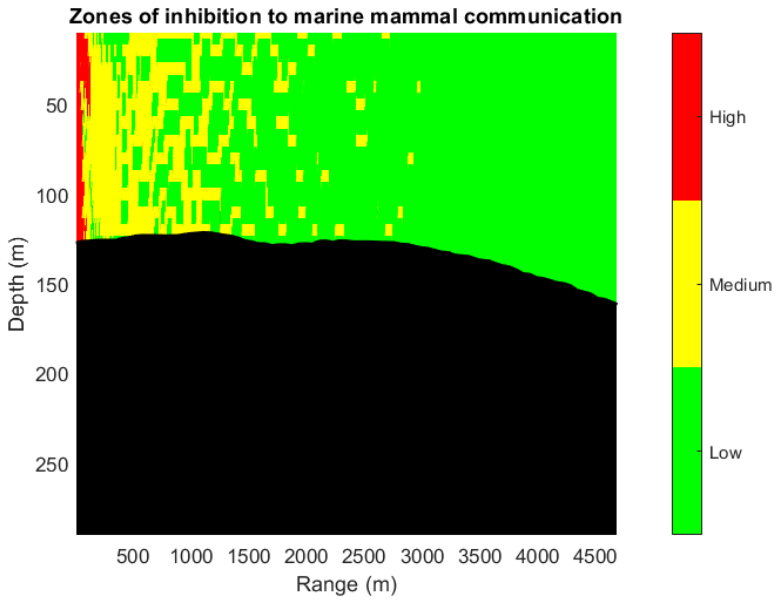

(b)

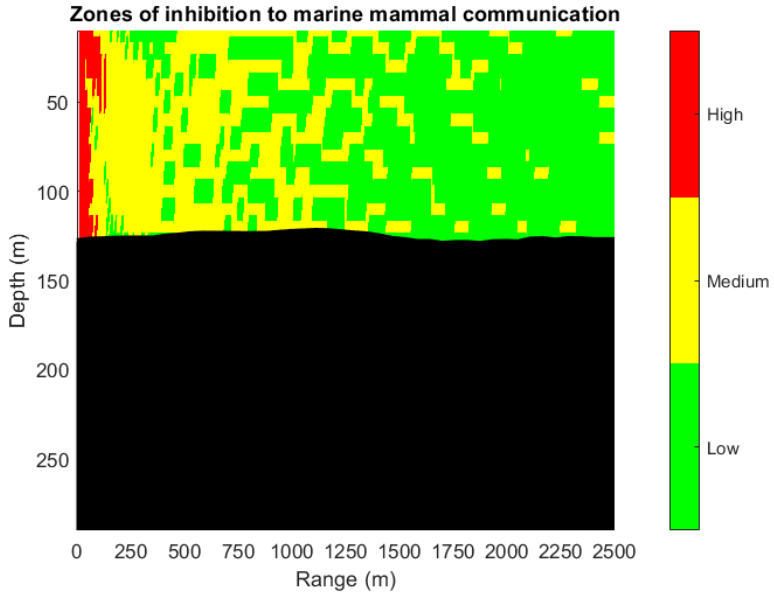

(c)

Figure 8: Transmission loss (a) and zones of inhibition to marine mammal communication (b) for simulation 1 with the seafloor adjusted so that the uppermost layer's shear velocity is reduced by one third from figure 4.(c) is a rescaled version of (b). The zones chosen for (b) and (c) are acquired from (a) by [0,17]TL – High, (17,33]TL – Medium and (33,+)TL – Low. The black portion in (b) and (c) is the seafloor. 0m depth is the ocean surface and positive depth is below the ocean surface (underwater).

7.4. Discussion

Figures 4-8 display the performance of the RAMGeo and RAMSGeo underwater acoustic propagation models. The transmission loss plots in figures 4(a)-8(a) seem to indicate that transmission loss is generally relatively low at points close to the noise source, which is mirrored in figures 2(b)-8(b) and their rescaled versions by the high-level zones of inhibition to marine mammal communication. Transmission loss appears to propagate in a wavey-like pattern. Time-domain signals were computed for simulations 3-4 and displayed in figures 6(c)-7(c), there are very minor differences between the RAMSGeo receiver signal and RAMGeo receiver signal, this is possibly due to the receiver location. There are stark differences in the transmission loss below the seafloor between RAMSGeo and RAMGeo, mainly transmission loss is higher beneath the seafloor in RAMSGeo, probably due to the shear mechanics.

The first (uppermost) layer of the seafloor was assumed to have the shear and compressive sound speeds of wet sand. The first layer's shear sound speed, a parameter unique to RAMSGeo, was altered from figure 4, and the results were displayed in figure 8 because multiple online sources estimate significantly different shear velocities for wet sand. Given that we do not have the actual seafloor parameters, it is important to know how well the model responds to the different estimates. It is also good to know how altering the shear forces, the only real difference between RAMSGeo and RAMGeo, affects acoustic propagation. Lowering the shear sound speed caused the medium zones of inhibition to propagate further in range, figure 8(b) vs figure 4(b), and made the RAMSGeo simulation's seawater acoustic dynamics further resemble those of the RAMGeo simulation displayed in figure 5(a).

The outer Bay of Fundy's seafloor layers' compressive sound speeds, shear sound speeds, densities, compressive attenuations, and shear attenuations are the final pieces of data needed to get a full accurate picture of the outer Bay of Fundy environment. The seafloor layers' parameter values used in the simulations are extremely rough approximations based on findings in various research papers and online sources not specific to the outer Bay of Fundy. These estimated seafloor parameters are most likely the largest source of controllable error in this modelling project. Until there is a completed dataset, perhaps it is best that we use RAMGeo because it requires less seafloor parameters, though this will come at the expense of dropping the effect of shear forces on acoustic propagation.

With the appropriate datasets, the two models appear to be capable of simulating underwater acoustic propagation in the outer Bay of Fundy for the purposes of studying the acoustic impact of shipping vessels to marine mammal communication. To accurately model the shipping and whale noise in the outer Bay of Fundy, we will need to know the frequencies that the ships and whales produce noise, as well as the depths at which the ships and whales are emitting the noise. The frequencies used to generate the simulations of this report are roughly based on common reported commercial shipping noises. Though the current values defining the inhibition zones are arbitrary, figures 4(b)-8(b) prove that it is possible to convert transmission loss plots into practical plots that clearly display zones of inhibition to marine mammal communication. To create accurate inhibition zones, we will need to know the noise tolerance levels for different marine mammal species in the outer Bay of Fundy. Though the computed signals at the arbitrary receiver locations defined in table 2, figures 6(c) and 7(c), are for a static sound source over multiple frequencies, it should be possible to approximate a moving shipping vessel by adjusting the frequencies according to the doppler effect and attaching time-domain receiver signals computed for multiple static sources along the ships trajectory together. The numerical simulations can

possibly be improved by working in smaller ranges to make the bathymetry and space grid more detailed, as well as further tuning the numerical parameters.

7.5. References

[1] “Assessment of Density Variations of Marine Sediments with Ocean and Sediment Depths”, R.Tenzer and V. Gladkikh, The Scientific World Journal, Hindawi Publishing Corporation ,2014.

[2] https://gpg.geosci.xyz/content/physical_properties/tables/seismic_velocity.html

[3] Physical Geology 2nd edition – open textbook “9.1 Understanding Earth Through Seismology”,

https://opentextbc.ca/physicalgeology2ed/chapter/9-1-understanding-earth-through-seismology/

[4] “Measurement and modeling of sound propagation over continental slope in the South China Sea”, Jin Liu et al, The Journal of the Acoustical Society of America, Acoustical Society of America, 2020.

[5] https://asa.scitation.org/doi/10.1121/1.1782932 (abstract).

8.0. Appendix B: *Additional communication inhibition zone model outputs*

All model outputs for North Atlantic Right Whales (NARW) and Humpback whales are included here. Not all figures are included here for Fin whales and Minke whales; excluded outputs showed entirely 'low' communication inhibition.

8.1. North Atlantic Right Whale (NARW)

All figures for NARW are included here.

8.1.1. Cruise ship

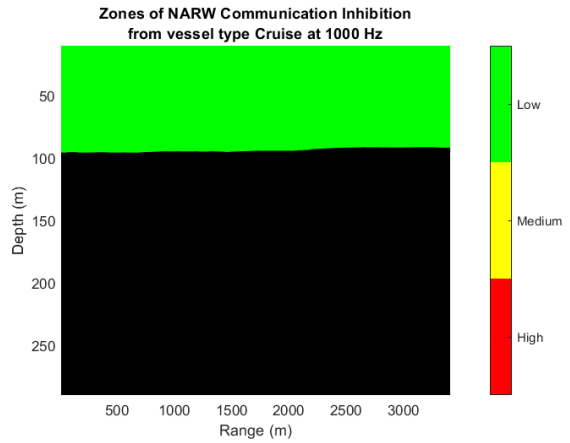

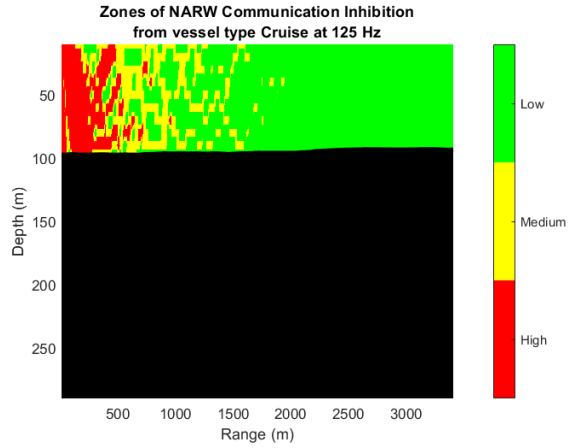

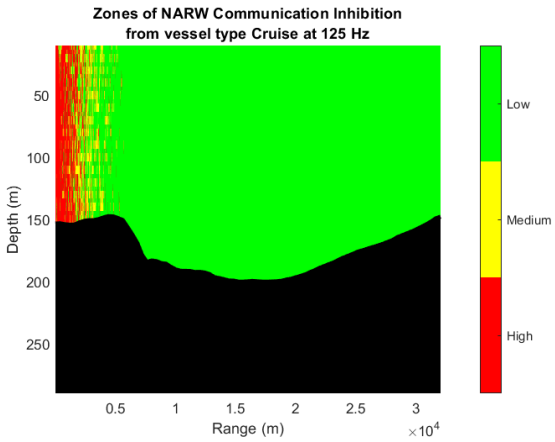

8.1.2. Container ship

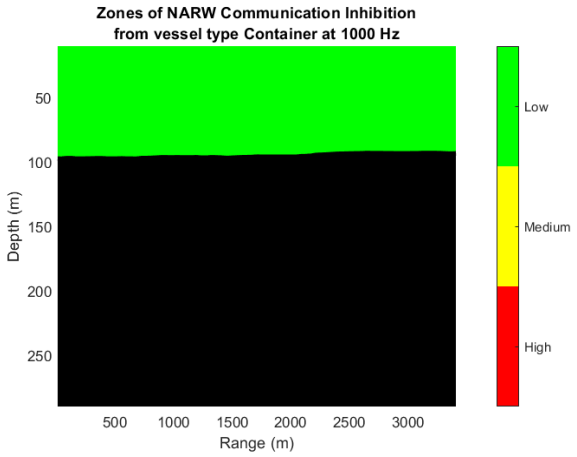

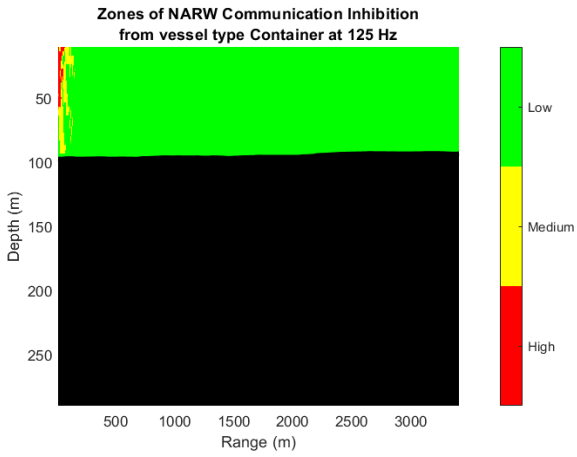

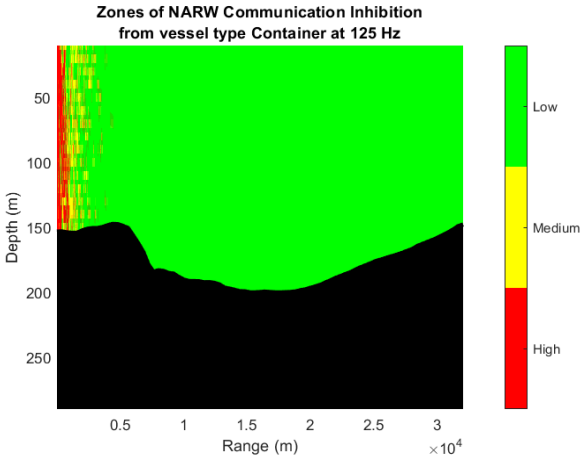

8.1.3. Potash ship

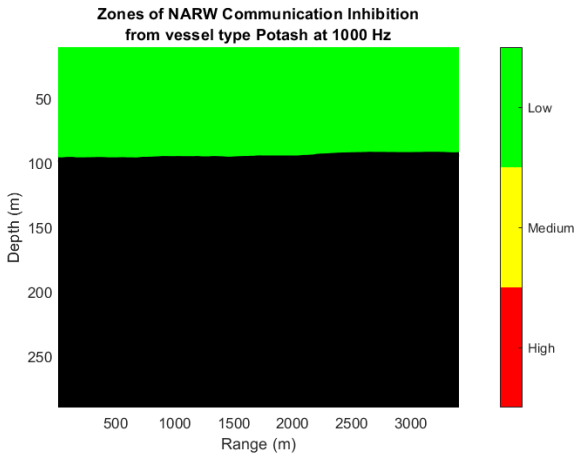

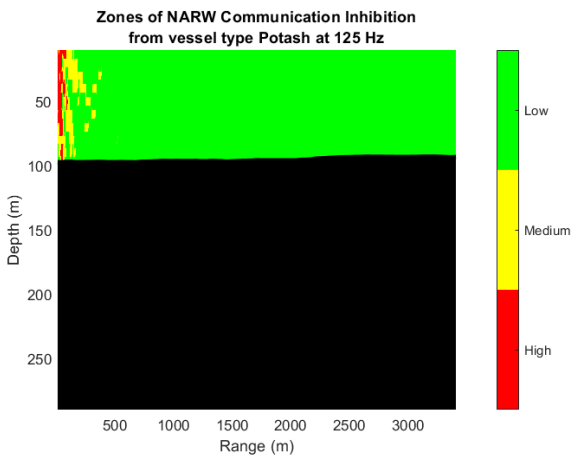

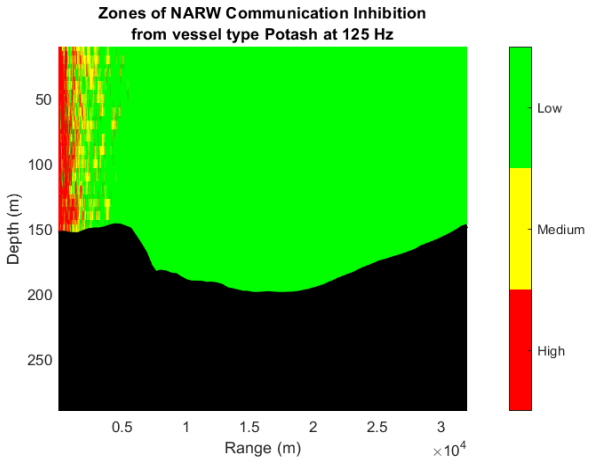

8.1.4. Petroleum ship

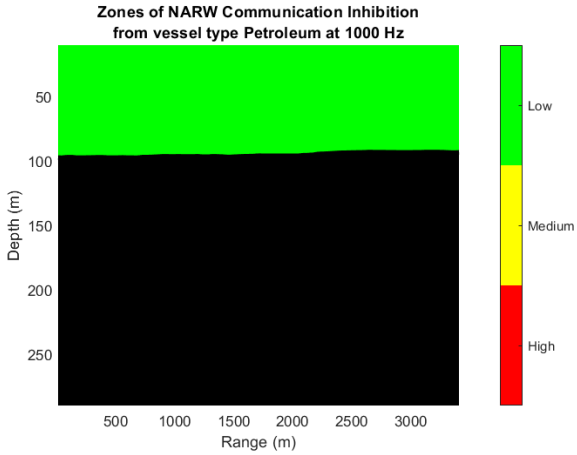

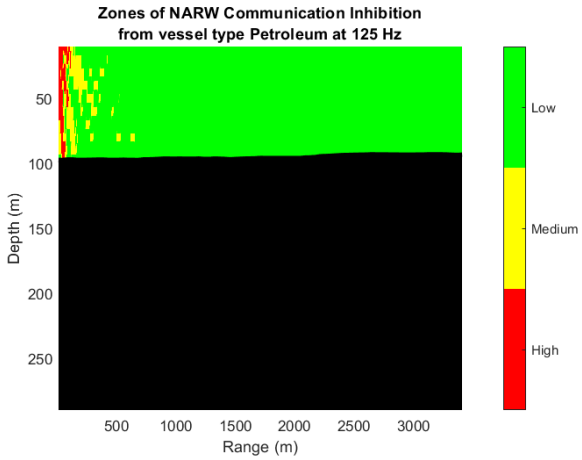

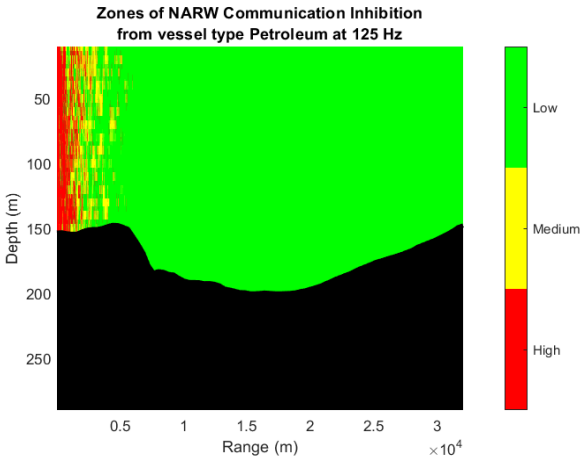

8.1.5. Crude oil ship

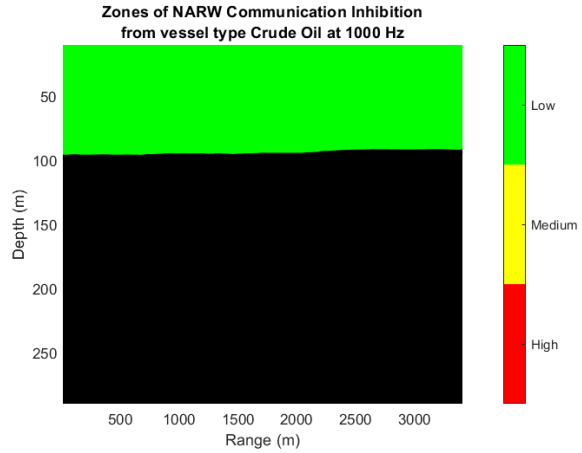

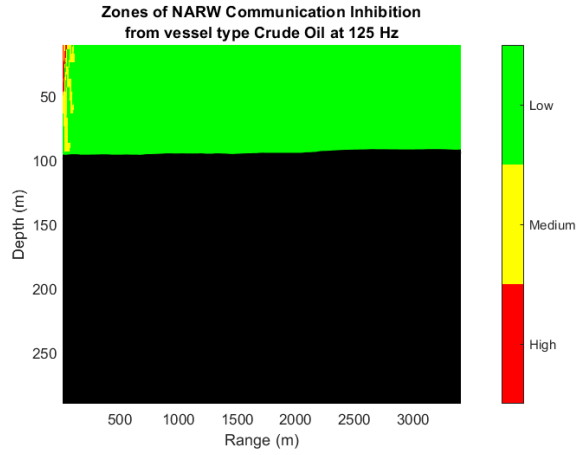

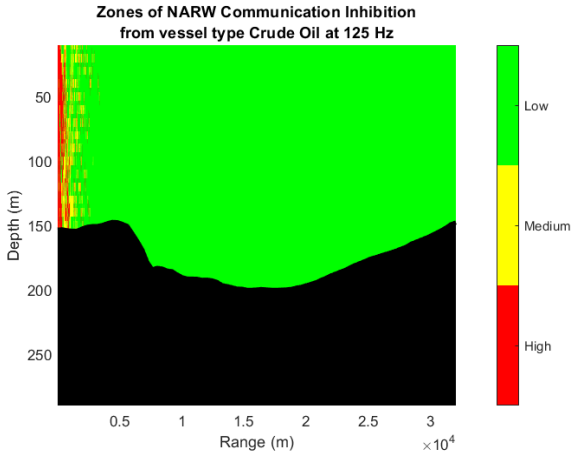

8.2. Humpback Whales

All figures for Humpback whales are included here.

8.2.1. Cruise ship

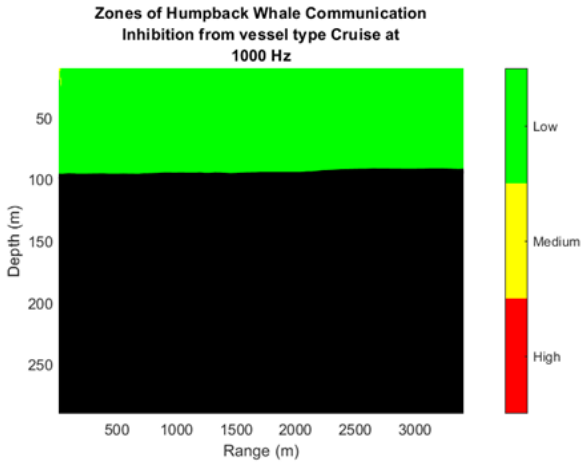

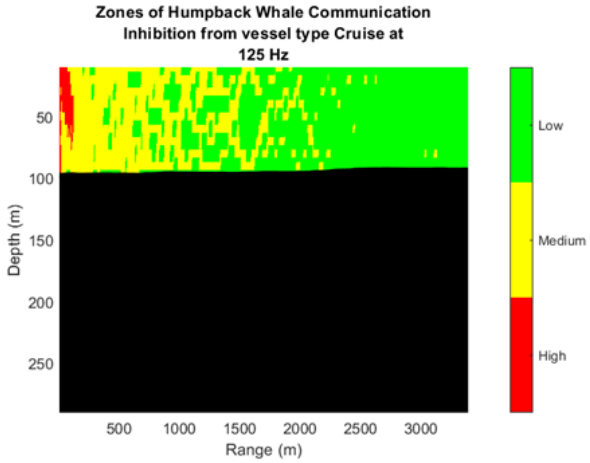

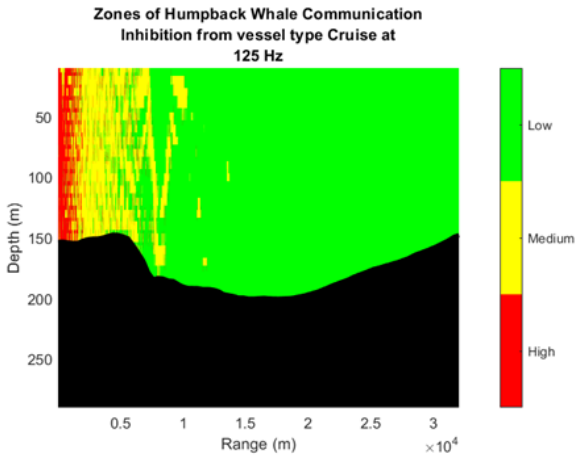

8.2.2. Container ship

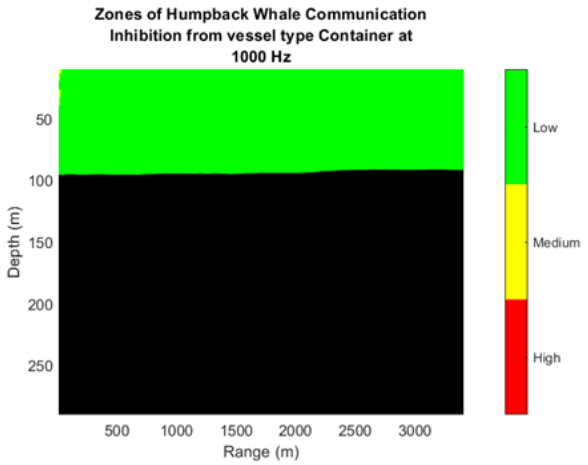

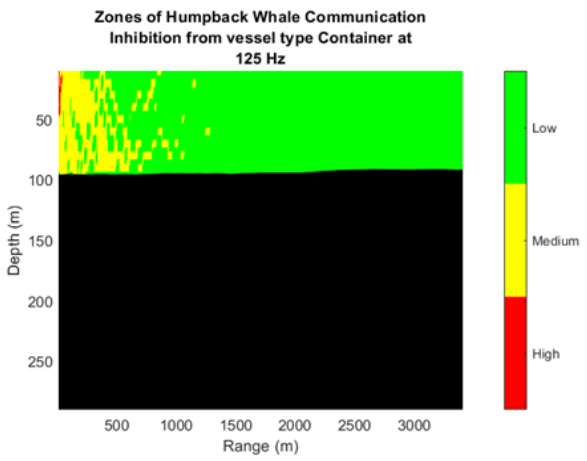

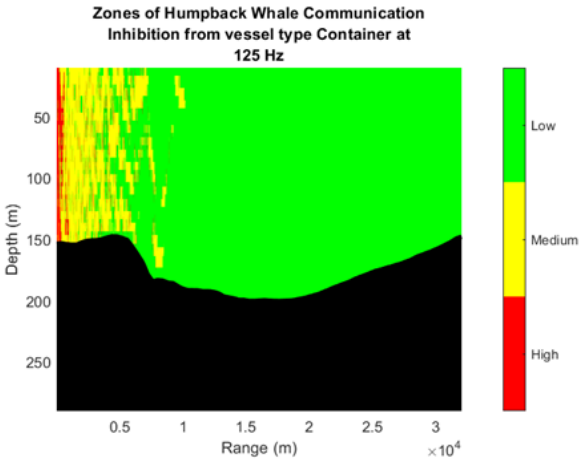

8.2.3. Potash ship

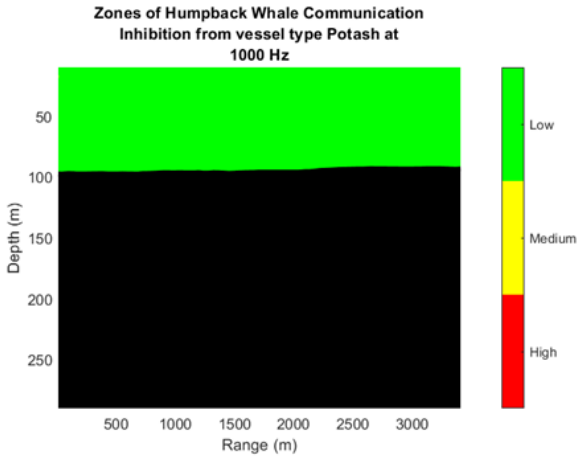

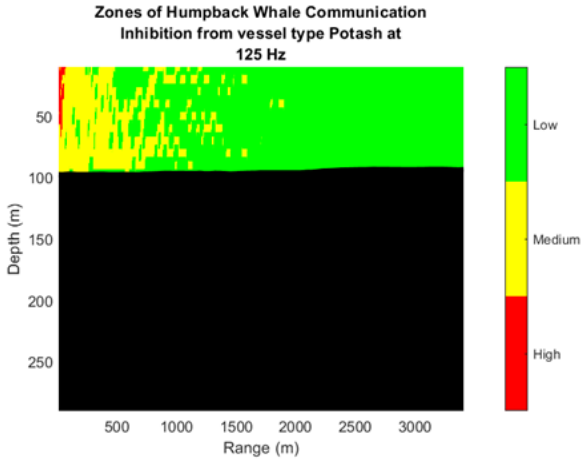

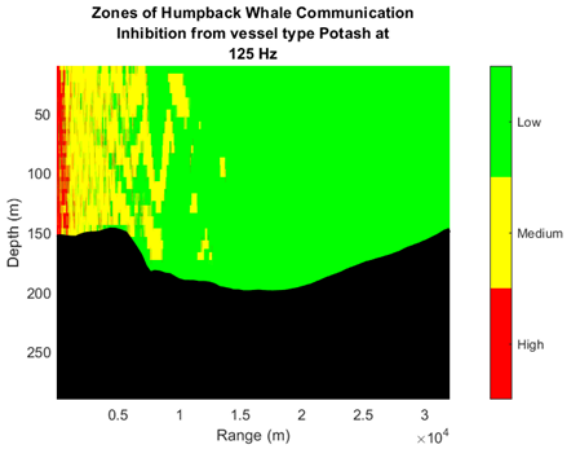

8.2.4. Petroleum ship

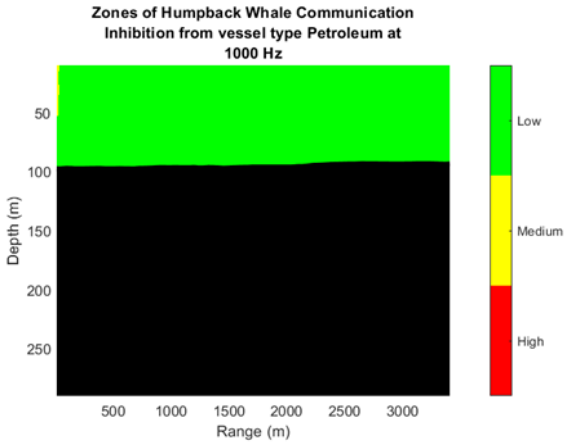

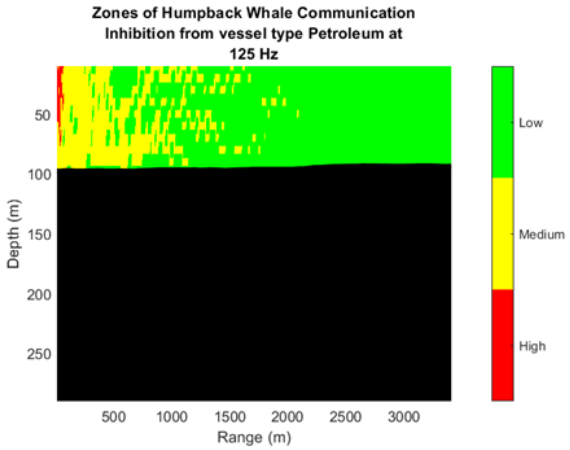

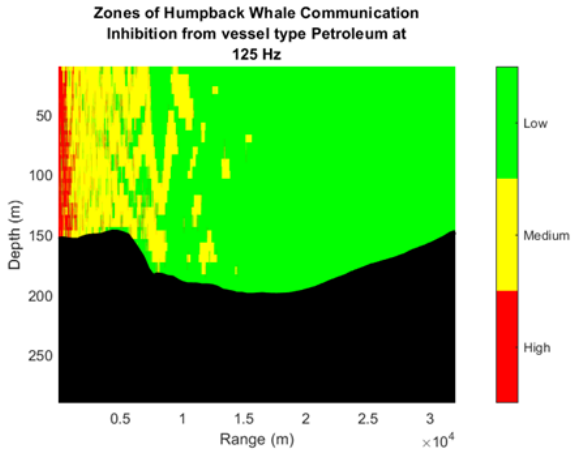

8.2.5. Crude oil ship

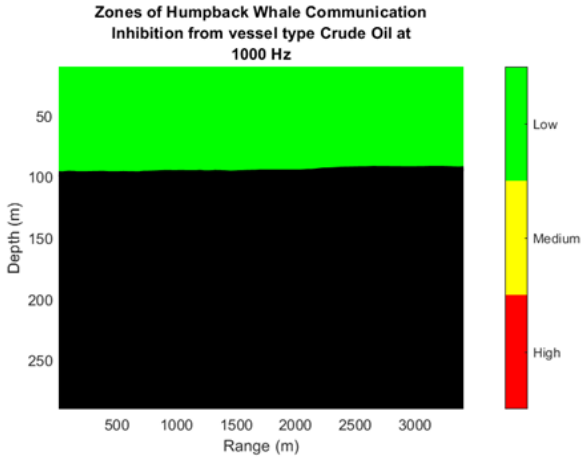

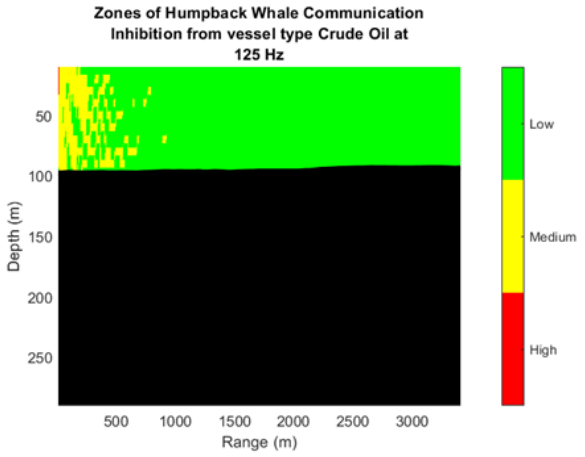

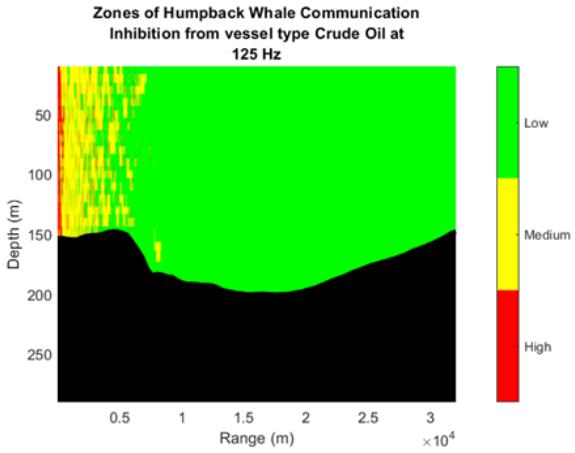

8.3. Fin Whale

Not included here: Container ships and crude oil ships at 125 Hz.

8.3.1. Cruise ship

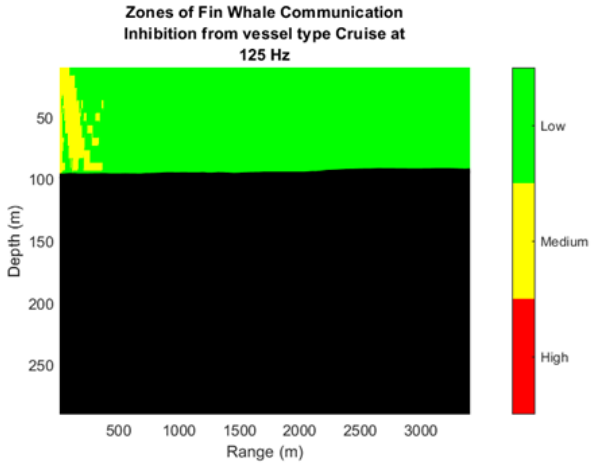

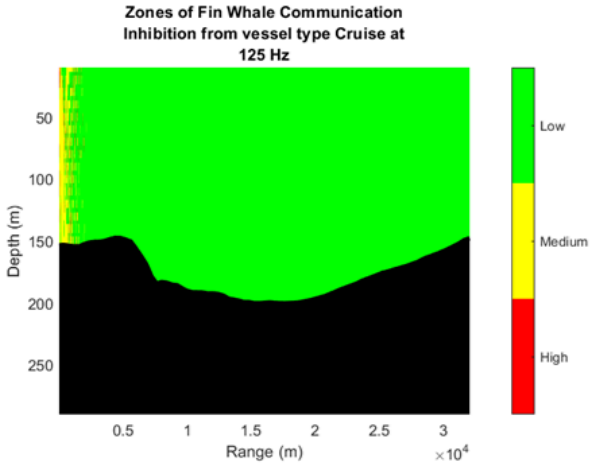

8.3.2. Petroleum ship

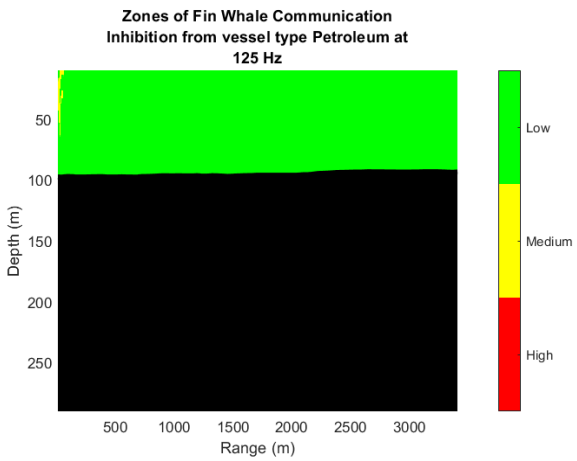

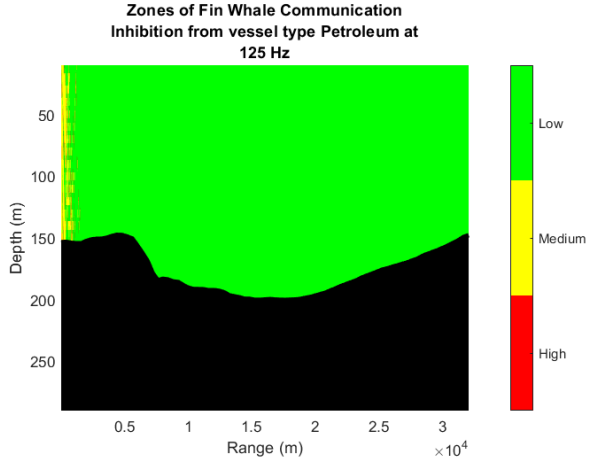

8.3.3. Potash ship

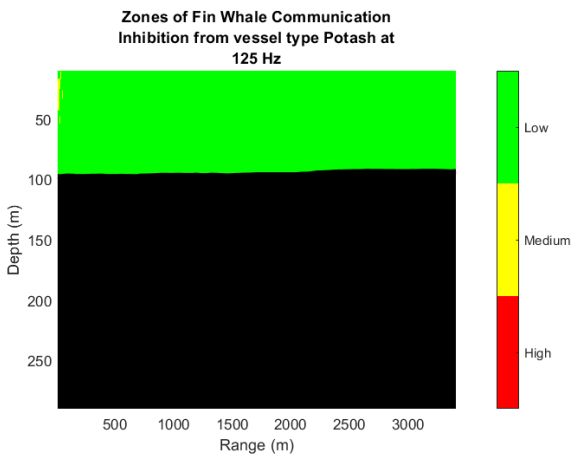

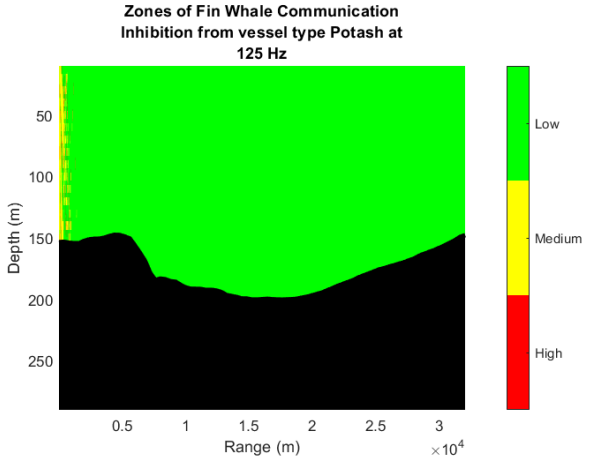

8.4. Minke Whale

Not pictured here: Container ship at 63 Hz, container ship at 125 Hz, container ship at 1000 Hz, crude oil ship at 63 Hz, crude oil ship at 125 Hz, crude oil ship at 1000 Hz, cruise ship at 63 Hz, cruise ship at 1000 Hz, petroleum ship at 63 Hz, petroleum ship at 1000 Hz, potash ship at 63 Hz, potash ship at 125 Hz, potash ship at 1000 Hz.

8.4.1. Cruise ship

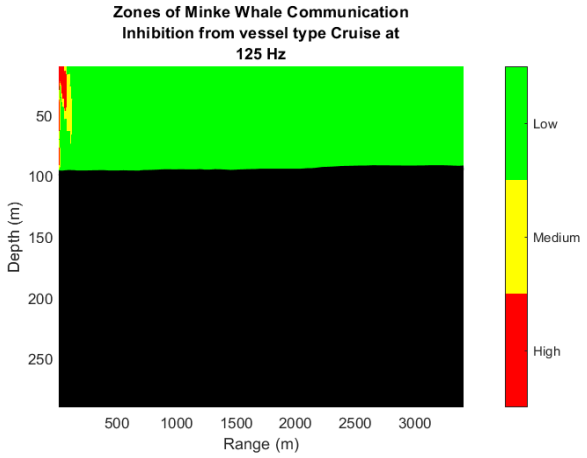

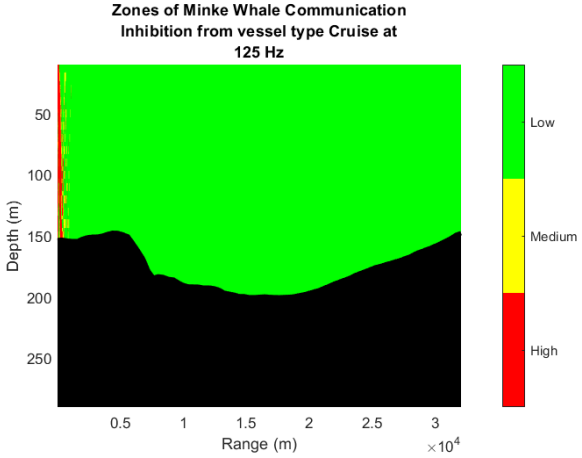

8.4.2. Petroleum ship

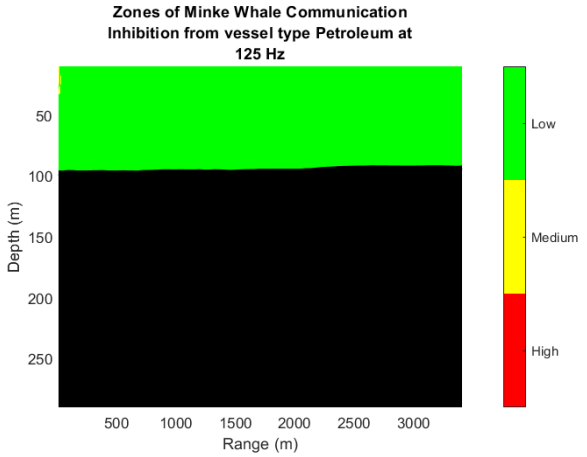

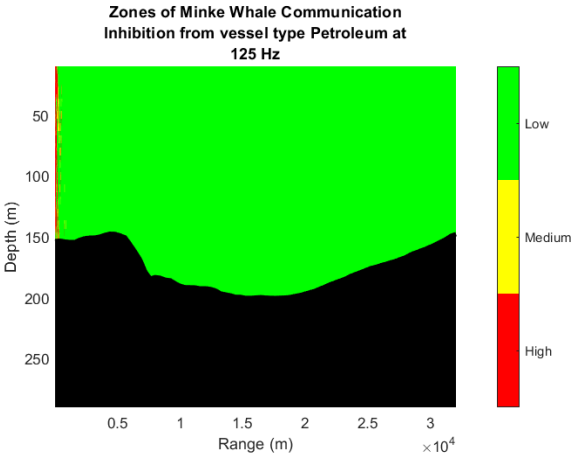

9.0. Appendix C: *Ship signatures*

Date, time, noise (in Hz) for five ⅓ octave bands, and vessel class of vessels leaving Port Saint John and passing by the passive acoustic monitoring hydrophone array adjacent to the Traffic Separation Scheme, confirmed through visual analysis. Values for noise are not yet adjusted for distance and depth away from the source of the noise (the vessel) which is done through the models created in this project. Ships which were not confirmed, for example by uncertainty caused be two ships passing by the hydrophone at the same time, are not included in this table.

Date	Time	20	63	125	1000	12500	Vessel Class
2021:10:08	234000	117.99	107.77	105.33	95.94	82.57	Container
2021:10:14	202000	96.6	108.04	114.47	102.9	95.67	Container
2021:10:15	194000	118.32	101.03	105.88	96.26	83.01	Container
2021:10:21	12000	78.23	96.2	102.68	90.95	79.87	Container
2021:10:22	230000	118	100.5	105.86	88	77.24	Container
2021:10:24	12000	113.02	109.31	104.3	95.45	82.99	Container
2021:10:29	200000	85.03	98	102.77	92.97	82.93	Container
2021:11:01	2000	117.04	105.17	106.96	95.47	82.59	Container
2022:08:10	222000	113.3	113.53	109.22	98.29	77.73	Container
2022:08:13	0	116.07	106.31	100.98	87.06	68.1	Container
2022:08:13	164000	119.51	105.96	106.54	94.7	72.57	Container
2022:08:18	50000	103.7	93.07	99.72	91.56	78.78	Container
2022:08:22	2000	113.45	100.52	103.41	94.64	77.69	Container
2022:08:22	80000	114.12	104.53	103.51	100.95	85.19	Container
2022:08:28	24000	112.3	100.15	105.44	100.11	77.91	Container
2022:08:31	192000	113.43	99.56	111.36	91.1	68.64	Container
2022:09:01	192000	112.46	105.51	107.46	98.78	85.54	Container

2022:09:02	222000	110.94	101.91	100.17	95.72	73.09	Container
2022:09:13	140000	104.01	95.2	100.99	83.65	68.31	Container
2022:09:15	24000	111.48	117	113.71	99.54	82.73	Container
2022:09:17	42000	111.19	105.63	101.89	95.65	80.78	Container
2022:09:21	120000	112.2	101.86	101.53	99.63	85.27	Container
2022:09:24	224000	109.38	102.12	106.67	102.11	84.82	Container
2022:09:28	30000	95.77	94.25	96.26	89.91	71.34	Container
2022:09:29	140000	106.73	102.76	103.52	94.72	78.27	Container
2022:09:30	164000	105.43	89.26	98.88	93.16	79.75	Container
2022:10:05	204000	84.42	95.72	98	93.94	73.8	Container
2022:10:08	102000	108.28	97.09	100.01	91.76	81.24	Container
2022:08:15	180000	118.74	117.64	109.6	93.71	74.4	Cruise
2022:08:30	200000	110.36	94.49	101.32	90.22	80.15	Cruise
2022:09:01	174000	107.75	104.94	109.9	100.3	81.75	Cruise
2022:09:04	180000	110.54	102.12	104.9	90.78	79.39	Cruise
2022:09:13	172000	118.23	107.53	106.06	101.85	81.24	Cruise
2022:09:15	172000	90.29	94.8	112.51	96.55	84.59	Cruise
2022:09:19	174000	115.33	91.91	103.14	98.18	78.72	Cruise
2022:09:21	204000	95.67	97.43	107.71	95.04	73.85	Cruise
2022:09:22	214000	106.81	103.05	102.39	95.07	88.3	Cruise
2022:09:25	234000	105.36	103.13	100.32	94.71	82.61	Cruise
2022:09:27	214000	111.97	88.46	105.38	86.39	77.8	Cruise

2022:09:28	162000	111.77	99.68	111.7	93.2	79.4	Cruise
2022:09:29	172000	110.59	97.33	108.3	99.24	81.35	Cruise
2022:09:30	20000	108.54	98.37	100.07	92.61	77.09	Cruise
2022:09:30	202000	108.56	93.13	100.49	93.08	81.94	Cruise
2022:10:04	180000	103.13	107.91	101.59	92.81	79.14	Cruise
2022:10:05	184000	108.74	97.6	99.58	87.53	75.53	Cruise
2022:10:05	194000	107.29	98.61	110.33	96.86	76.86	Cruise
2022:10:06	210000	107.49	91	103.63	92.22	76.39	Cruise
2021:10:08	32000	120.74	98.28	116.05	87.56	78.63	Oil - Petroleum
2021:10:09	24000	93.05	103.04	113.22	101.01	83.45	Oil - Petroleum
2021:10:10	32000	79.56	101.27	103.06	89.1	72.86	Oil - Petroleum
2021:10:11	0	119.91	99.97	102.31	92.53	75.6	Oil - Crude
2021:10:11	42000	85.49	96.85	102	97.26	83.99	Oil - Petroleum
2021:10:12	62000	116.18	112.52	111.67	103.83	89.88	Oil - Petroleum
2021:10:13	200000	119.43	110.37	112.17	98.72	83.9	Oil - Petroleum
2021:10:14	194000	84.63	103.11	109.05	98.56	80.31	Oil - Petroleum
2021:10:15	90000	84.74	112.1	115.32	94.06	81.41	Oil - Petroleum
2021:10:15	104000	120.08	100.07	103.91	84.37	74.69	Oil - Crude
2021:10:16	112000	119.49	99.51	114.56	88.73	81.17	Oil - Petroleum
2021:10:16	222000	84.06	103.09	102.15	93.61	82.56	Oil - Petroleum
2021:10:17	232000	88.32	98.16	98.53	91.9	79.92	Oil - Petroleum
2021:10:18	114000	88.64	108.92	110.21	98.39	84.79	Oil - Petroleum

2021:10:20	140000	117.05	98.53	108.08	99.3	83.1	Oil - Petroleum
2021:10:21	132000	79.76	109.61	102.13	95.78	82.39	Oil - Petroleum
2021:10:22	10000	99.96	101.69	101.96	88.04	76.41	Oil - Crude
2021:10:23	40000	118.43	107.64	106.61	98.1	83.43	Oil - Petroleum
2021:10:23	160000	117.77	99.91	121.03	92.6	80.65	Oil - Petroleum
2021:10:25	30000	93.09	112.15	114.2	95.42	84.5	Oil - Petroleum
2021:10:26	54000	114.89	107.64	105.35	93.76	83.47	Oil - Petroleum
2021:10:27	62000	109.71	99.3	110.97	98.82	87.58	Oil - Petroleum
2021:10:28	60000	89.42	101.75	110.49	101.64	86.77	Oil - Petroleum
2021:10:29	192000	79.43	98.71	108.16	97.85	83.42	Oil - Petroleum
2021:10:30	212000	108.4	110.01	103.88	97.34	84.6	Oil - Petroleum
2021:10:31	102000	115.69	105.01	112.55	97.37	89.71	Oil - Petroleum
2021:11:01	222000	87.25	103.72	102.92	96.72	85.78	Oil - Petroleum
2022:08:10	210000	119.29	106.09	105.81	97.86	78.74	Oil - Crude
2022:08:11	0	95.07	109.56	115.5	104.25	85.19	Oil - Petroleum
2022:08:12	34000	116.23	97.09	105.13	75.87	67.58	Oil - Crude
2022:08:12	140000	115.34	98.08	97.12	94.67	74.06	Oil - Petroleum
2022:08:12	144000	116.41	102.47	107.13	95.98	74.69	Oil - Petroleum
2022:08:14	64000	117.46	103.65	101.61	86.19	80.68	Oil - Crude
2022:08:14	142000	105.52	107.14	118.92	108.51	89.45	Oil - Petroleum
2022:08:14	160000	114.89	112.3	112.04	90.56	71.85	Oil - Petroleum
2022:08:15	42000	114.48	108.8	110.31	99.51	84.53	Oil - Petroleum

2022:08:16	32000	102.92	100.94	107.2	95.76	76.07	Oil - Petroleum
2022:08:16	52000	114.07	102.95	103.49	91.43	75.1	Oil - Petroleum
2022:08:17	182000	113.4	105.02	105.06	98.8	90.43	Oil - Petroleum
2022:08:18	184000	97.63	108.47	111.67	96.44	82.66	Oil - Petroleum
2022:08:19	190000	83.34	101.13	111.75	91.42	75.33	Oil - Petroleum
2022:08:19	202000	112.9	100.08	110.26	101.67	82.6	Oil - Petroleum
2022:08:20	22000	110.57	107.12	98.81	89.7	71.33	Oil - Crude
2022:08:20	200000	90.56	103.76	110.93	100.88	81.51	Oil - Petroleum
2022:08:23	104000	92.18	110.58	116.8	103.78	87.73	Oil - Petroleum
2022:08:23	190000	114.34	100.73	100.54	85.26	70.71	Oil - Crude
2022:08:24	0	111.54	112.67	116	107.19	89.58	Oil - Petroleum
2022:08:25	120000	86.47	96.6	104.06	99.36	80.3	Oil - Petroleum
2022:08:25	194000	115.54	96.97	98.68	84.5	70.4	Oil - Crude
2022:08:27	10000	98.49	106.82	110.01	96.74	79.96	Oil - Petroleum
2022:08:27	130000	74.93	102.79	108.08	90.79	76.87	Oil - Petroleum
2022:08:30	30000	96.73	105.71	115.28	102.99	84.75	Oil - Petroleum
2022:08:30	164000	113.07	98.99	103.8	94.31	81.12	Oil - Petroleum
2022:08:30	184000	114.83	104.74	105.19	91.96	82.93	Oil - Crude
2022:09:01	170000	97.68	105.37	115.13	102.04	85.26	Oil - Petroleum
2022:09:02	42000	95.39	107.91	109.5	108.06	88.13	Oil - Petroleum
2022:09:02	210000	113.86	101.89	103.55	88.04	70.54	Oil - Crude
2022:09:04	70000	95.59	100.5	109.53	97.11	77.77	Oil - Petroleum

2022:09:04	204000	113.69	110.86	111.7	88.1	73.03	Oil - Petroleum
2022:09:13	160000	109.17	106.39	114.42	101.48	85.03	Oil - Petroleum
2022:09:14	160000	81.07	106.35	110.06	92.51	81.12	Oil - Petroleum
2022:09:15	180000	112.86	102.77	117.5	95.08	84.28	Oil - Petroleum
2022:09:17	60000	81.71	114.39	113.55	99.37	86.41	Oil - Petroleum
2022:09:17	72000	110.45	102.55	111.45	102.04	85.34	Oil - Petroleum
2022:09:17	134000	106.84	97.63	106.58	84.63	70	Oil - Crude
2022:09:18	64000	78.37	100.37	110.39	106.58	87.43	Oil - Petroleum
2022:09:21	94000	73.19	103.02	106.92	94.31	80.03	Oil - Petroleum
2022:09:21	100000	79.1	110.77	112.15	96.65	79.26	Oil - Petroleum
2022:09:22	110000	77.86	108.92	104.53	100.13	85.85	Oil - Petroleum
2022:09:22	124000	110.31	101.2	106.55	94.94	84.09	Oil - Petroleum
2022:09:23	2000	110.91	96.68	107.52	104.05	84.48	Oil - Petroleum
2022:09:23	122000	90.37	94.93	106.76	100.03	82.67	Oil - Petroleum
2022:09:23	134000	115.9	109.21	110.49	91.74	82.58	Oil - Petroleum
2022:09:26	82000	113.38	95.02	98.15	92.51	81.14	Oil - Crude
2022:09:26	124000	77.05	88.63	99.67	91.84	81.01	Oil - Petroleum
2022:09:28	144000	77.09	101.7	105.75	95.28	81.23	Oil - Petroleum
2022:09:30	4000	111.37	98.1	99.55	89.76	77.67	Oil - Crude
2022:09:30	40000	70.3	92.12	83.11	83.97	76.36	Oil - Petroleum
2022:10:03	64000	84.25	104.99	109.56	96.58	83.29	Oil - Petroleum
2022:10:05	94000	102.29	97.06	100.62	99.19	82.86	Oil - Petroleum

2022:10:07	120000	105.48	103.54	104.61	97.83	86.57	Oil - Petroleum
2022:10:07	124000	110.12	96.99	100.06	89.06	72.96	Oil - Crude
2022:10:08	0	102.74	111.59	105.79	96.57	85.2	Oil - Petroleum
2022:10:08	110000	95.97	100.26	101.67	97.15	84.74	Oil - Petroleum
2021:10:12	44000	100.36	99.12	100.35	94.3	84.49	Other: recycled metal
2021:10:15	220000	99.64	110.91	107.39	100.47	88.37	Potash
2021:10:18	232000	87.27	100.17	100.21	92.77	90.3	Other: fish oil
2021:10:29	74000	84.44	98.52	111.38	94.21	84.34	Potash
2022:08:12	10000	92.14	88.82	101.64	74.77	66.72	Potash
2022:08:13	12000	85.74	92.27	107.25	90.16	70.49	Potash
2022:08:19	70000	95.07	111.3	107.57	92.44	80.4	Other: recycled metal
2022:08:24	222000	104.12	98.78	107.42	93.27	67.36	Other: equipment
2022:08:30	34000	110.4	111.03	109.72	95.18	81.07	Potash
2021:10:25	42000	95.62	95.42	107.69	98.63	84.96	Tug

10.0. Appendix D: *Call parameters*

Call parameters for marine mammals which were used in the calculation and visualization of zones of communication inhibition.

10.1. Humpback whale (*Megaptera novaeangliae)*

Humpback whale (*Megaptera novaeangliae*) calling behavior in Southeast Alaska: a study in acoustic ecology and noise (Fournet 2018).

- Mean call source level was 137 dB @ 1m, with values ranging from 127 – 173 dBRMS re 1 µPa @ 1 m
    - However, Glacier Bay NPP has limited vessel traffic
- As ambient sound levels rose in the bandwidth of a humpback's call, they increased their source call levels by 0.1 dB for every 1 dB increase in ambient noise
    - Probability of calling also decreased 10% for every 1 dB increase in ambient sound
    - Probability of calling was 25-30% lower when noise was vessel noise vs ambient noise

Maximum source levels were 162– 171 dB for low-frequency pulse trains from a visible feeding whale (Thompson et al. 1986).

- Feedback to this paper shows some assumptions were made incorrectly (now with more knowledge) and these estimates may be slightly high

Source levels of social sounds in migrating humpback whales (*Megaptera novaeangliae*) (Dunlop et al. 2013).

- Median levels (rms): 158 dB

Best hearing sensitivity 120 Hz - 4 kHz (Erbe 2002).

10.2. North Atlantic Right Whale (*Eubalaena glacialis*)

An overview of North Atlantic right whale acoustic behavior, hearing capabilities and responses to sound (Matthews & Parks, 2021).

- Upcall: 147 - 154 (rms, dB re 1 µPa-m, 50 Hz to 10 kHz).

Should be most sensitive to sounds 100-400 Hz based on their vocalizations (Erbe 2002).

10.3. Fin Whale (*Balaenoptera physalus*)

Should be sensitive to sounds 20-150 Hz based on their vocalizations (Erbe 2022).

Estimated source levels of fin whale vocalizations: Adjustments for surface interference (Charif et al. 2002).

- Recordings from Oregon and Northern California
- Estimated source levels with adjustments for spherical spreading loss had a median of 171 dB, with a range of 159-184 dB

Source Levels of 20 Hz Fin Whale Notes Measured as Sound Pressure and Particle Velocity from Ocean-Bottom Seismometers in the North Atlantic (Pereira et al. 2021).

- Average source level was 196.9 dB re 1 µPa m for the seismometer (derived from particle velocity measurements) and 186.7 dB re 1 µPa m for the hydrophone.

Source levels of fin whale 20 Hz pulses measured in the Northeast Pacific Ocean (Weirathmueller et al. 2013)

- Average source level of 189 +/- 5.8 dB re 1 µPa at 1 m.

10.4. Minke Whale (*Balaenoptera acutorostrata*)

Minkes appear most sensitive between 100-200 Hz, with good sensitivity extending from 60 Hz-2 kHz. High-frequency clicks were published in two studies, indicating some sensitivity between 4-7.5 kHz, up to 20 kHz (Erbe 2002).

Individual calling behaviour and movements of North Atlantic minke whales (*Balaenoptera acutorostrata*) (Risch, Siebert & Van Parijs, 2014).

- Average source levels (SLrms) for minke whales pulse trains ranged between 164 and 168 dB re 1 µPa, resulting in a minimum detection range of 0.4–10.2 km for these calls in a coastal environment.

10.5. References

Erbe, 2002. Hearing abilities of baleen whales. Defence Research & Development Canada, Contract Report. https://cradpdf.drdc-rddc.gc.ca/PDFS/unc09/p519661.pdf

Charif, R. A., Mellinger, D. K., Dunsmore, K. J., Fristrup, K. M., & Clark, C. W. (2002). Estimated source levels of fin whale (*Balaenoptera physalus*) vocalizations: Adjustments for surface interference. *Marine Mammal Science*, *18*(1), 81-98.

Fournet, M. E. (2018). Humpback whale (*Megaptera novaeangliae*) calling behavior in Southeast Alaska: a study in acoustic ecology and noise. (Chapter 5: Source levels of foraging Humpback whale calls)

Pereira, A.; Romagosa, M.; Corela, C.; Silva, M.A.; Matias, L. Source Levels of 20 Hz Fin Whale Notes Measured as Sound Pressure and Particle Velocity from Ocean-Bottom Seismometers in the North Atlantic. J. Mar. Sci. Eng. 2021, 9, 646. https://doi.org/10.3390/ jmse9060646

Risch, D., Siebert, U., & Van Parijs, S. M. (2014). Individual calling behaviour and movements of North Atlantic minke whales (Balaenoptera acutorostrata). *Behaviour*, *151*(9), 1335-1360.

M. H. Rasmussen, M. Lammers, K. Beedholm, L. A. Miller; Source levels and harmonic content of whistles in white-beaked dolphins (*Lagenorhynchus albirostris*). *J Acoust Soc Am* 1 July 2006; 120 (1): 510–517. https://doi.org/10.1121/1.2202865

Matthews, L, Parks, S. (2021) An overview of North Atlantic right whale acoustic behavior, hearing capabilities and responses to sound. *Mar Pol Bul*. 173. 10.1016/j.marpolbul.2021.113043

Dunlop, R. A., Cato, D. H., Noad, M. J., & Stokes, D. M. (2013). *Source levels of social sounds in migrating humpback whales (Megaptera novaeangliae). The Journal of the Acoustical Society of America, 134(1), 706–714.* doi:10.1121/1.4807828